Bottom-up solutions to plasma synthesis of nanomaterials

R. Mohan Sankaran

George B. Mayer Assistant Professor of Engineering
Department of Chemical Engineering
Case Western Reserve University
Cleveland, OH 44106-7217
Email: mohan@case.edu
http://microplasma.case.edu

Plasma processing of materials

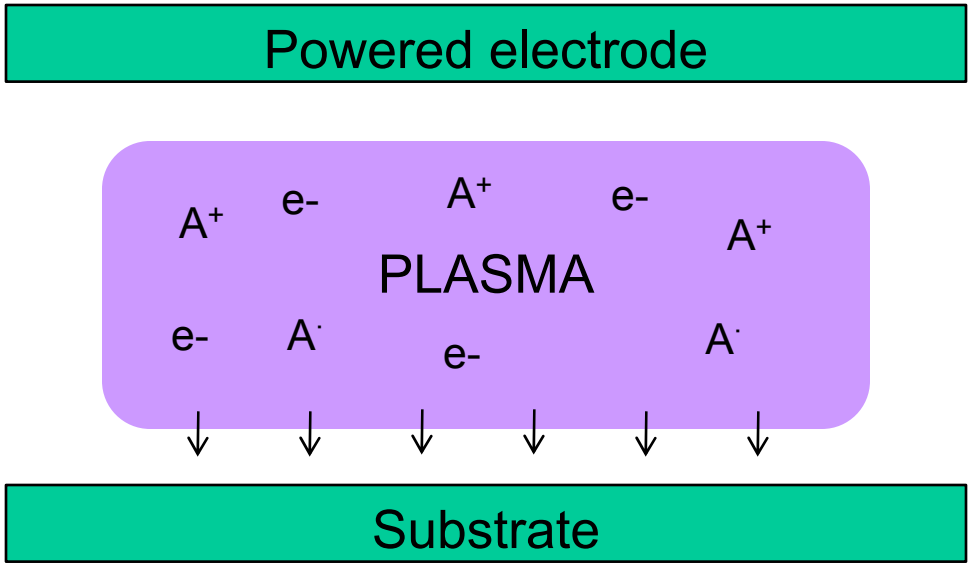

- High purity
- High fidelity pattern transfer
- Low temperature processing
- Large volume (large area)

Plasma etching of Si

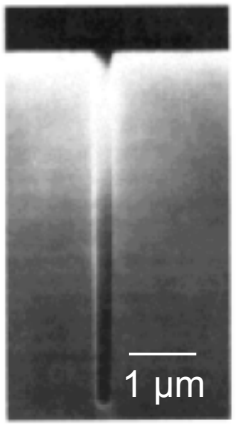

Applied Materials, Inc.

Plasma-enhanced CVD of amorphous Si

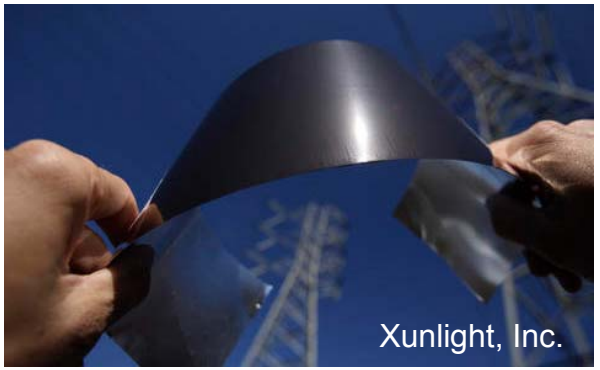

From top-down approaches to…

2007 2010 ?

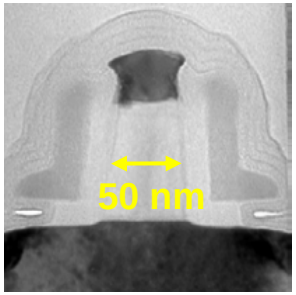

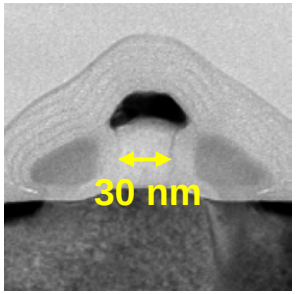

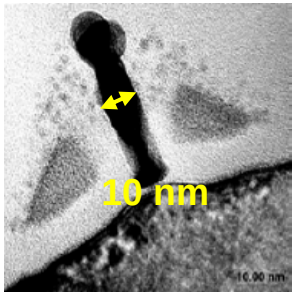

Manufacturing Research Development

Chau *et al.*, Intel (2007)

…to bottom-up approaches to materials synthesis

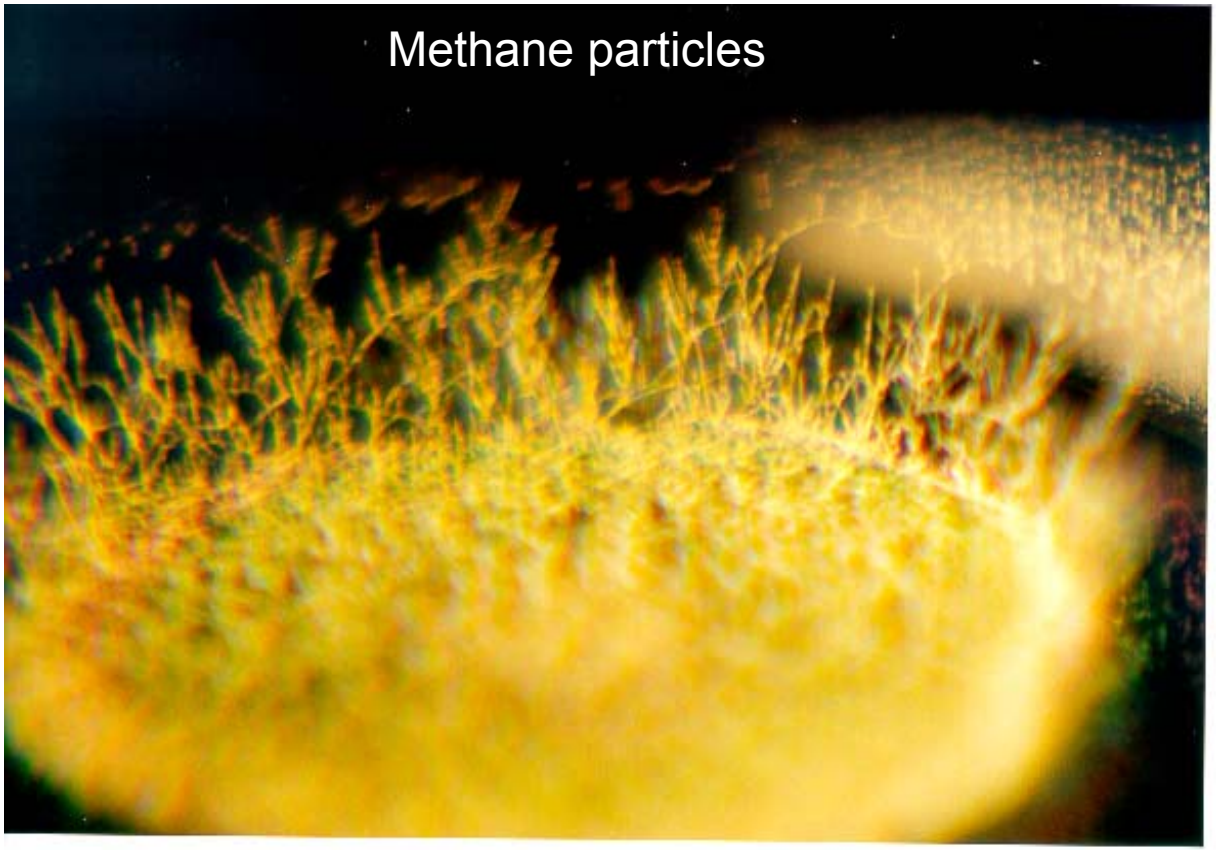

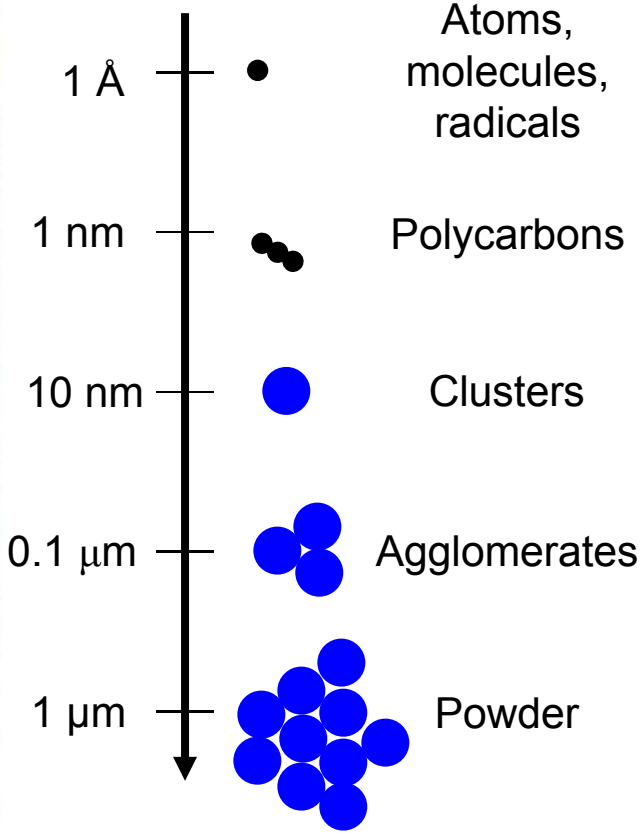

Stoffels *et al.*, J. Vac. Sci. Technol. A , Vol. 17, 3385 (1999)

A new direction for plasma synthesis of materials

Conventional plasma

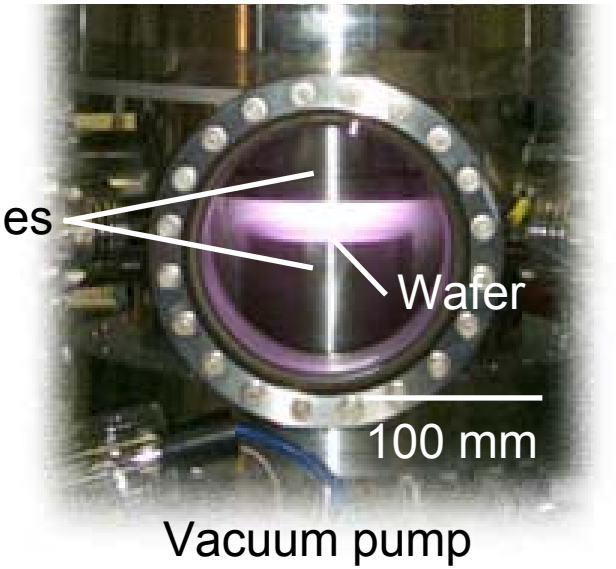

- Large volume, batch
- Low pressure (10^{-5}-1 Torr)
- Non-thermal [> 10,000 K]
- Plasma-surface interactions

Microplasma

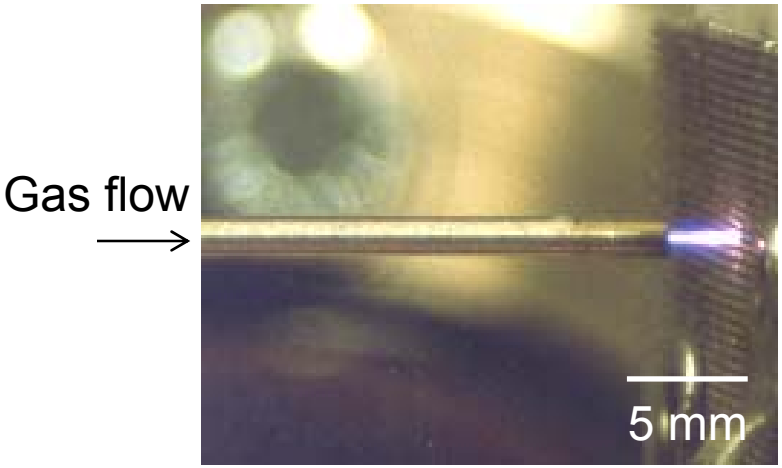

- Microscale, continuous-flow
- High pressure (10-1000 Torr)
- Non-thermal [> 10,000 K]
- Gas-phase interactions

Microplasmas are a versatile source for nanomaterials synthesis

Gas-phase nucleation of nanoparticles

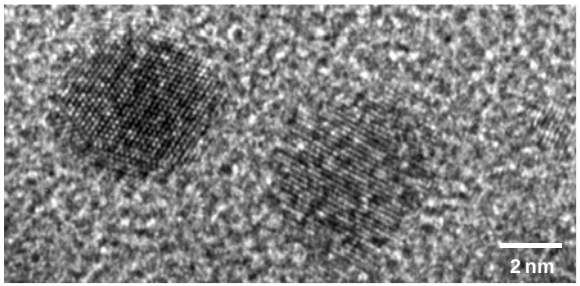

Chiang *et al.*, APL **91**, 121503 (2007)
Chiang *et al.*, Adv. Mater **20**, 4857 (2008)

Plasma-liquid electrochemistry

Richmonds *et al.*, APL **93**, 131501 (2008)
Chiang *et al.*, PSST, in press

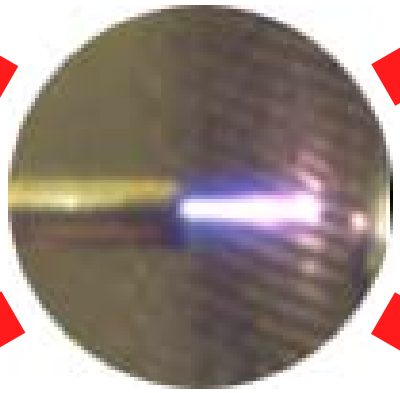

Catalytic growth of well-defined CNTS

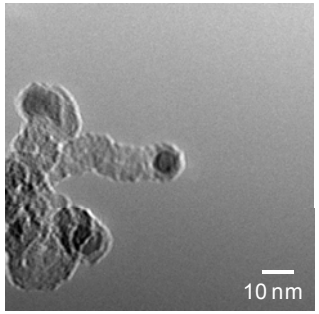

Chiang *et al.*, JPCC **112**, 17920 (2008)
Chiang *et al.*, Diam. Rel. Mater. **18**, 946 (2009)
Chiang *et al.*, Nature Mater. **8**, 882 (2009)
Chiang *et al.*, ACS Nano, ASAP online

Non-lithographic micro/nanofabrication

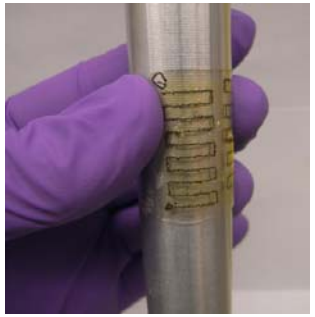

Chiang *et al.*, APL **91**, 021501 (2007)
Lee *et al.*, in preparation

Microplasmas operate stably and continuously at atmospheric pressure

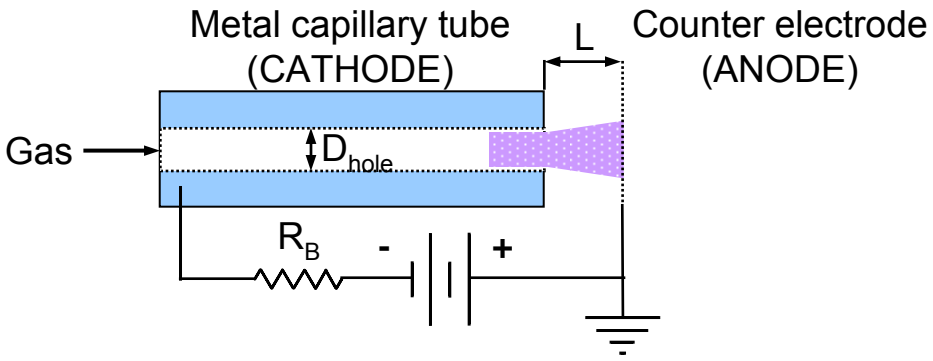

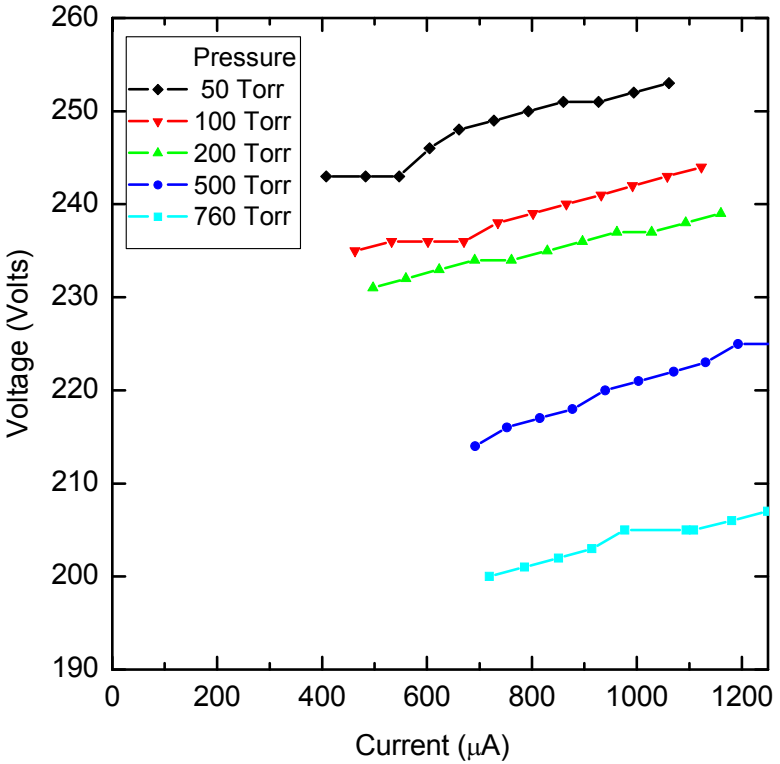

Typical operating conditions (for single discharge):

- *100 sccm Ar*
- *V_{plasma}=450 V DC, I_{plasma}=5 mA*
- *D_{hole}=180 μm, L=2 mm*

Continuous atmospheric-operation in Ar gas flow for at least 100 hrs!

U.S. Patent No. 6,700,329 (Issued 3/2/04)

Gas-phase nucleation of nanoparticles

Batch vs. continuous-flow synthesis of nanoparticles: The example of CdSe

Batch

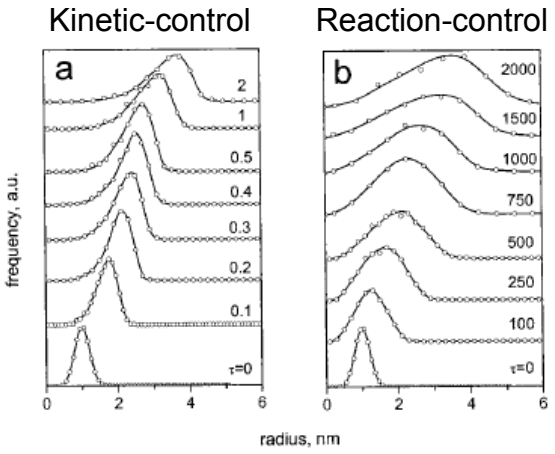

Talapin *et al.*, J. Phys. Chem. B, Vol. 105, 12278 (2001)

Continuous-flow

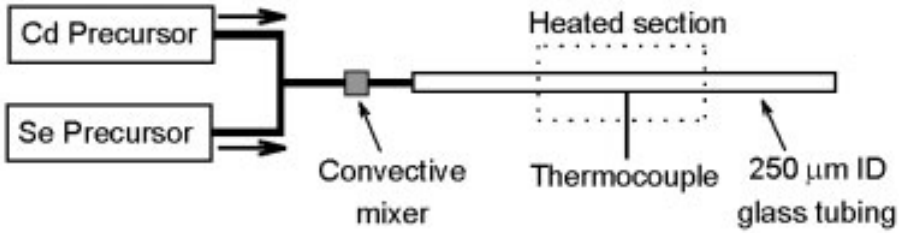

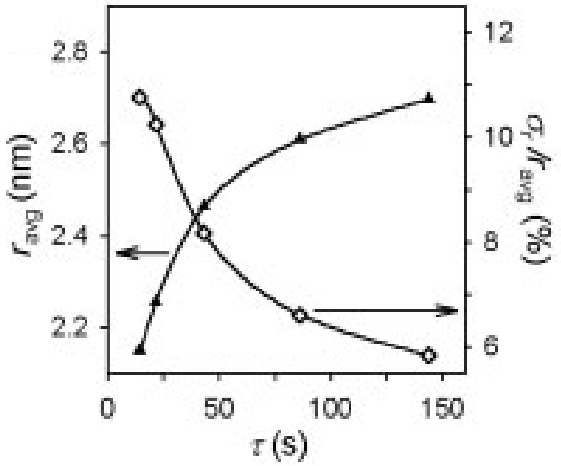

Yen *et al.*, Adv. Mater., Vol. 15, 1858 (2003)

Continuous-flow microreactors based on microplasmas

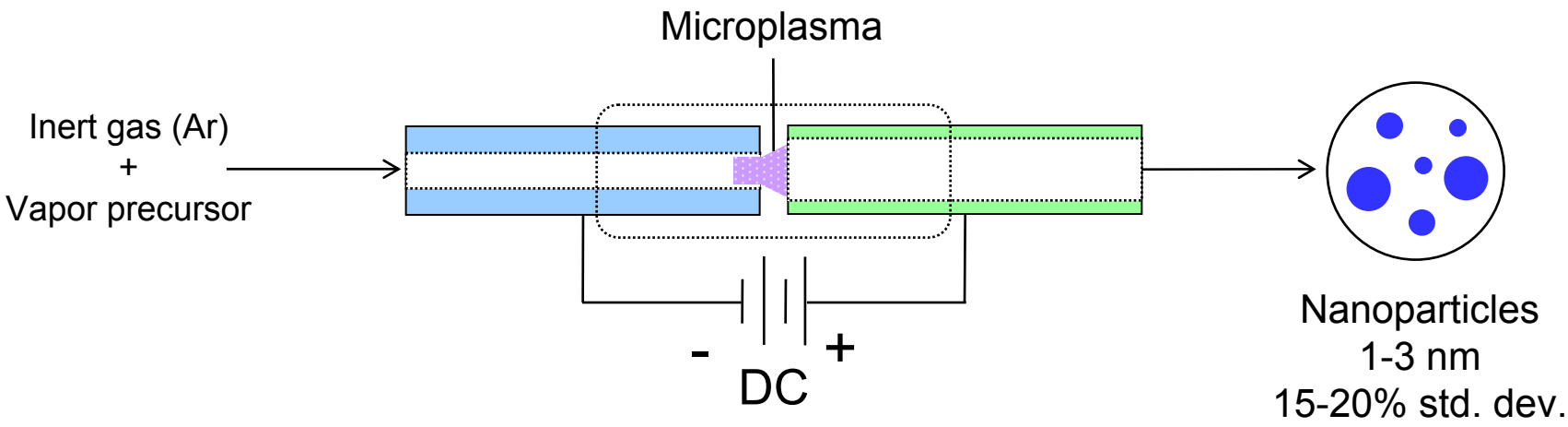

Characteristics of process

- Non-thermal dissociation of reactive precursor molecules (EID)
- Short residence times (10^{-3}-10^{-6} seconds)
- *In situ* monitoring (kinetic studies)
- Generic – precursor can be chosen to grow different materials

Continuous-flow synthesis and *in situ* size classification of nanoparticles

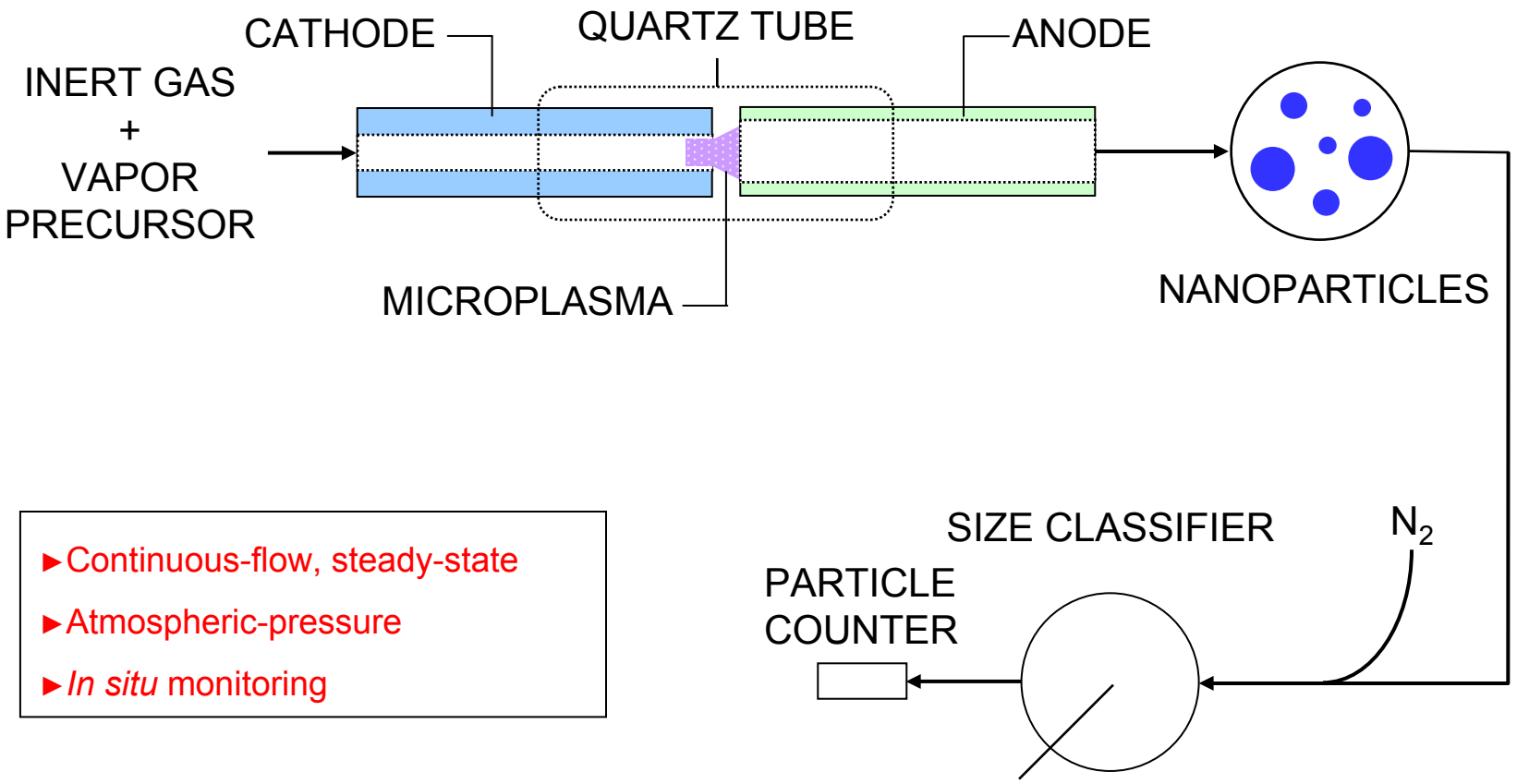

- ►Continuous-flow, steady-state
- ►Atmospheric-pressure
- ►*In situ* monitoring

Cylindrical differential mobility analyzer (TSI, Inc.)

Detects particles 2 nm < D_p < 100 nm

Aerosol measurements of Fe and Ni nanoparticles

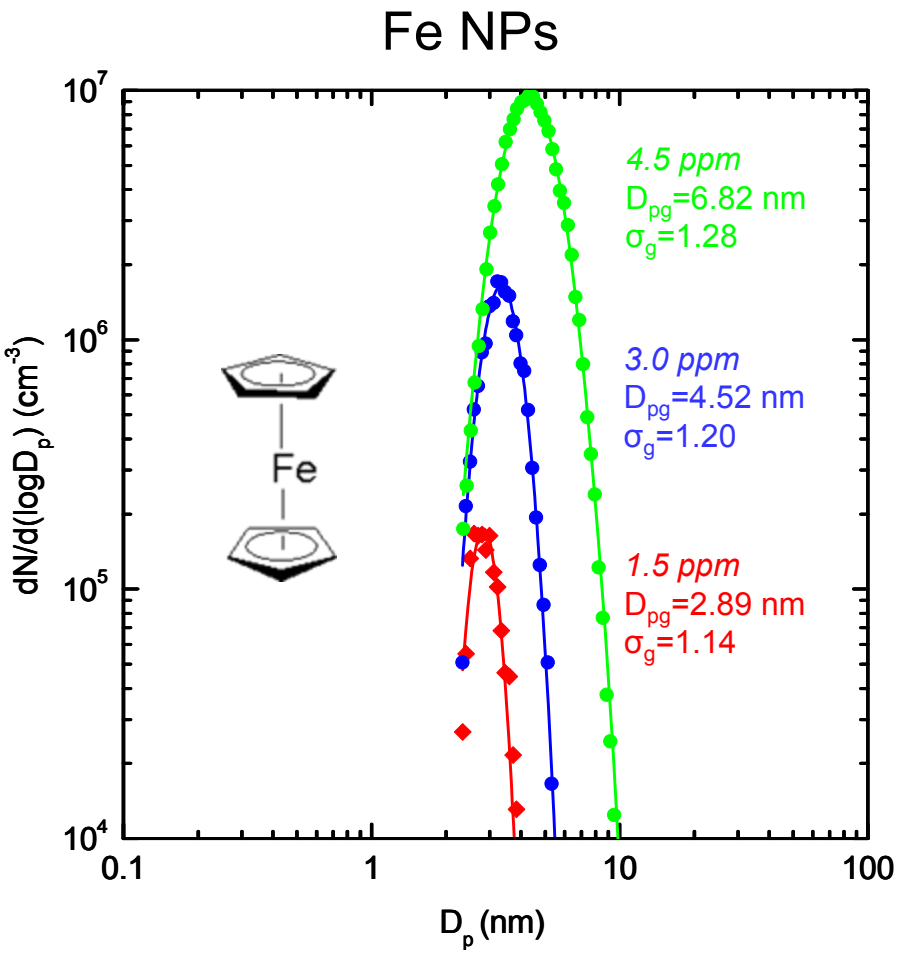

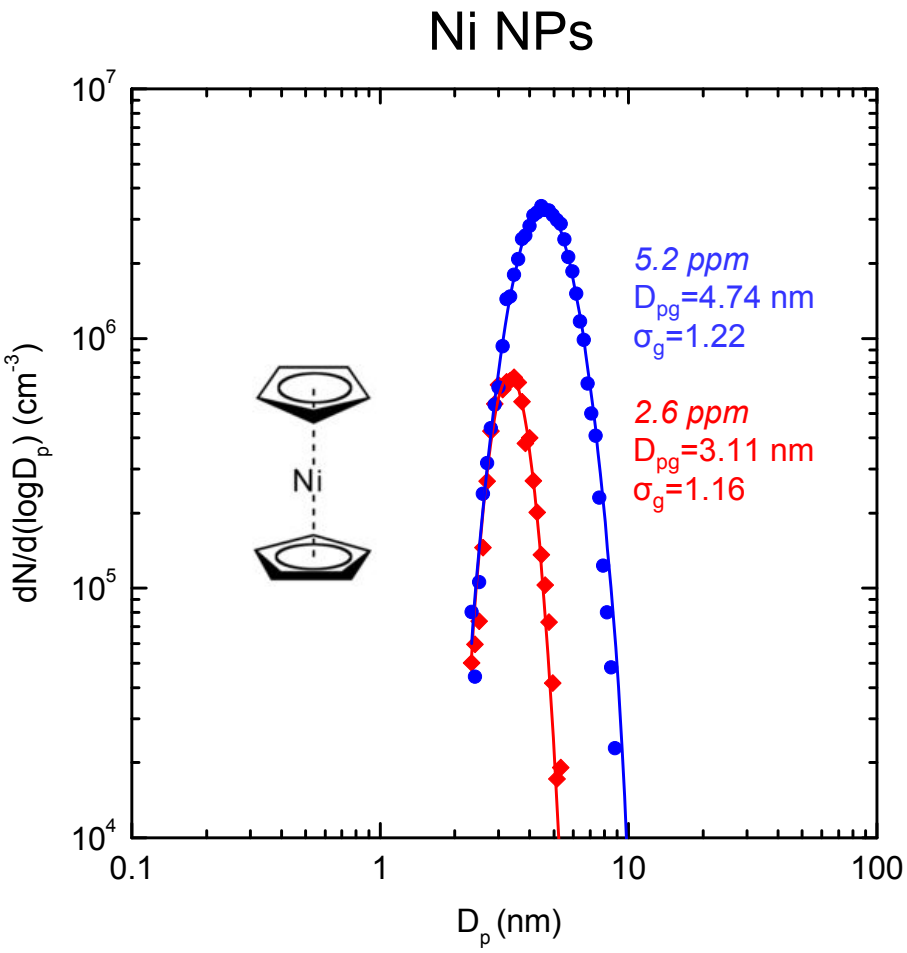

Mechanism for nucleation and growth of NPs from vapor-phase precursors

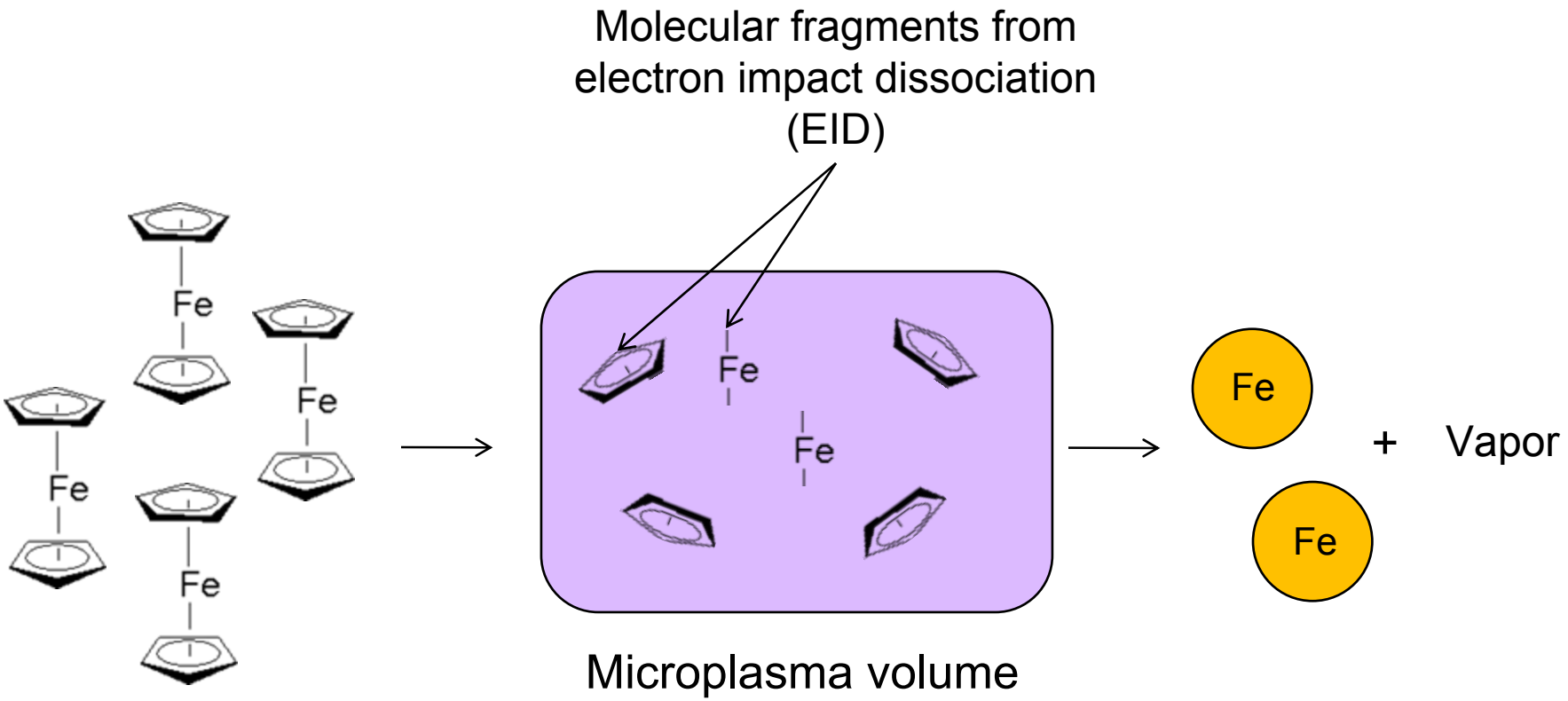

►For constant plasma parameters, D_p is a function of precursor concentration and enthalpy of dissociation

►ΔH_D(ferrocene) ~ 662 kcal/mol; ΔH_D(nickelocene) ~ 686 kcal/mol

HRTEM analysis of as-grown Ni nanoparticles deposited by electrostatic precipitation

2.0 ppm

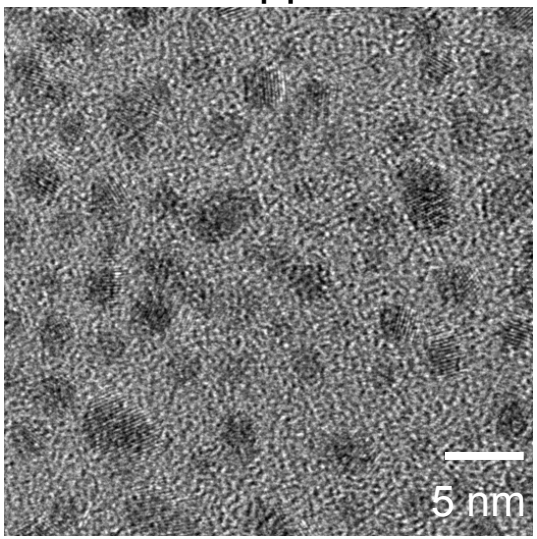

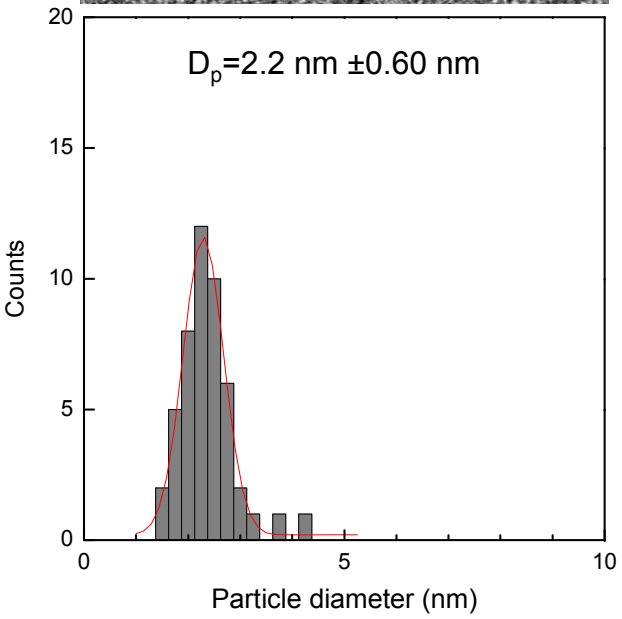

2.6 ppm

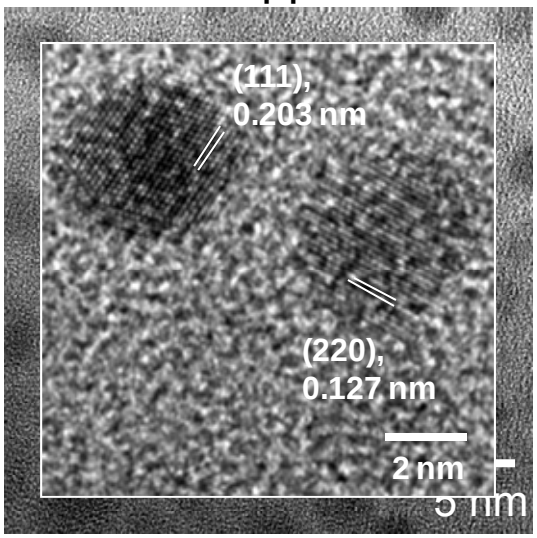

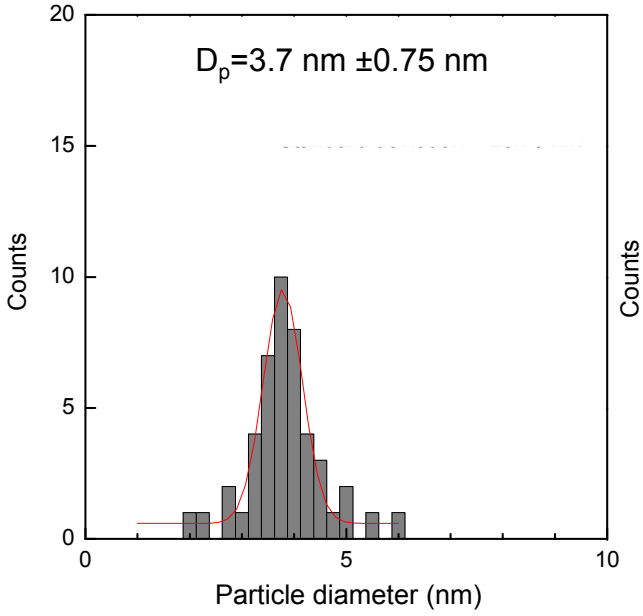

5.2 ppm

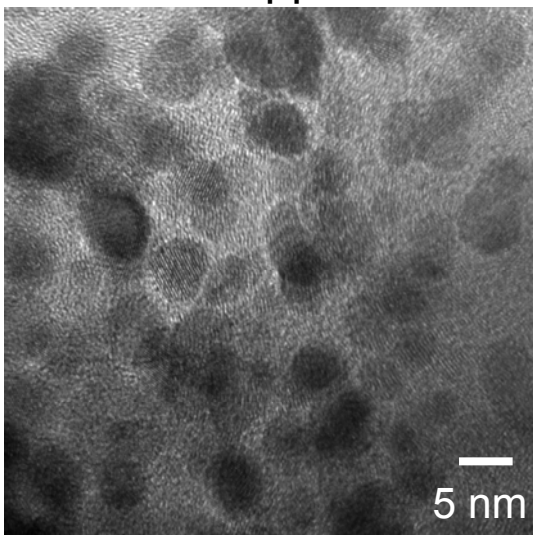

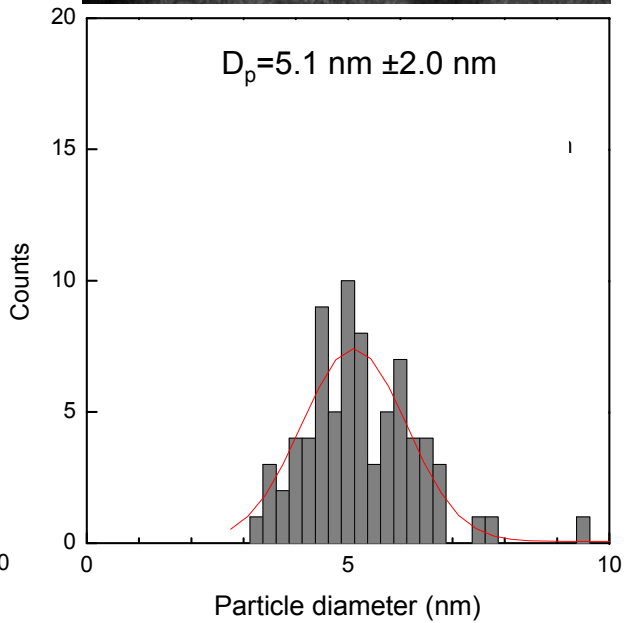

Compositionally-controlled growth of bimetallic (alloyed) nanoparticles

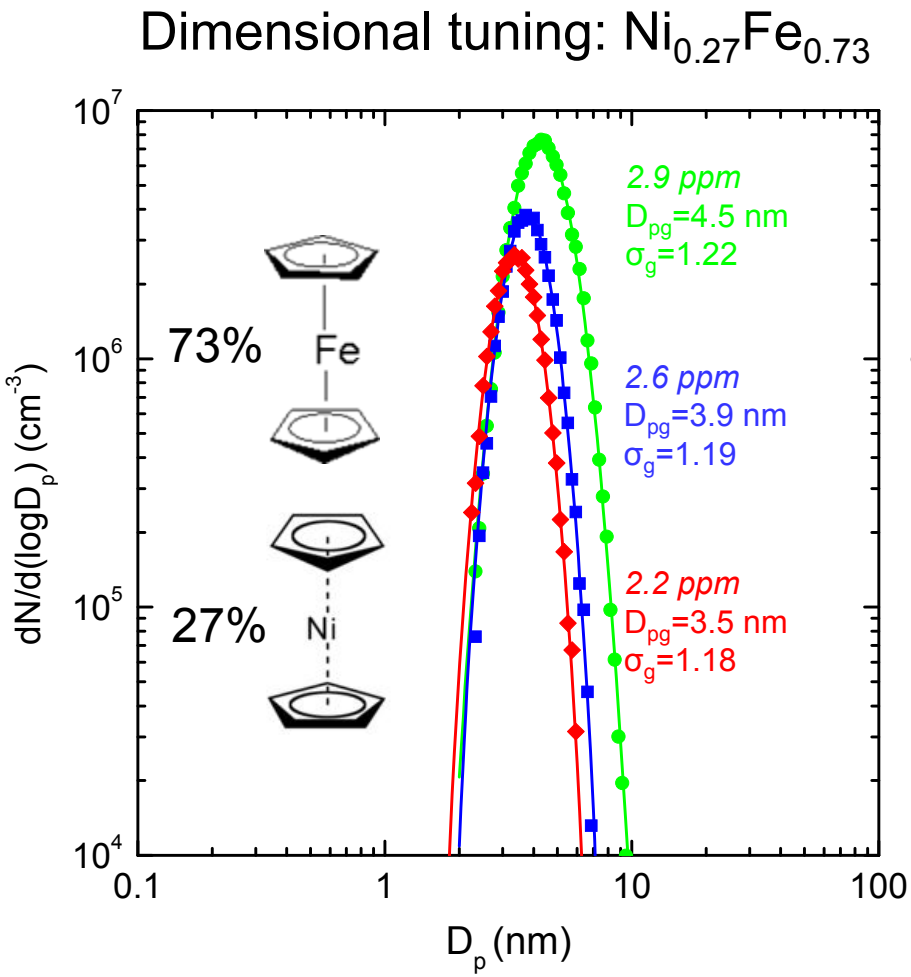

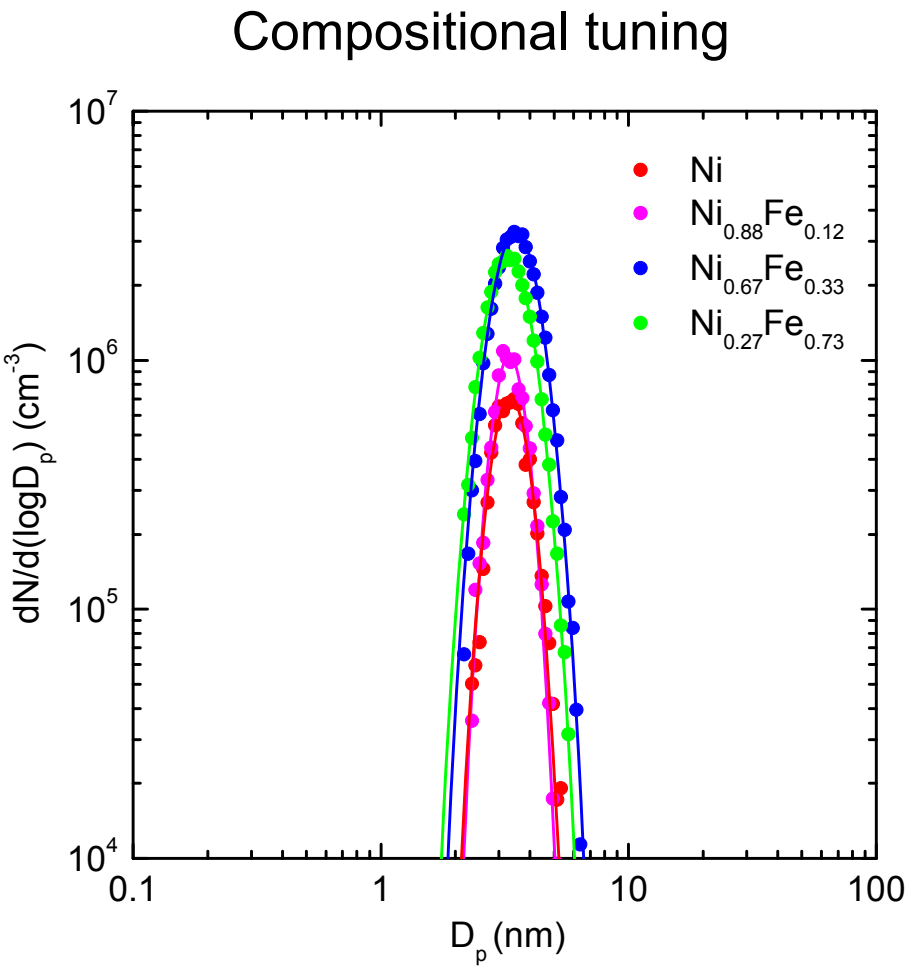

EDS of as-grown Ni_xFe_{1-x} bimetallic nanoparticles

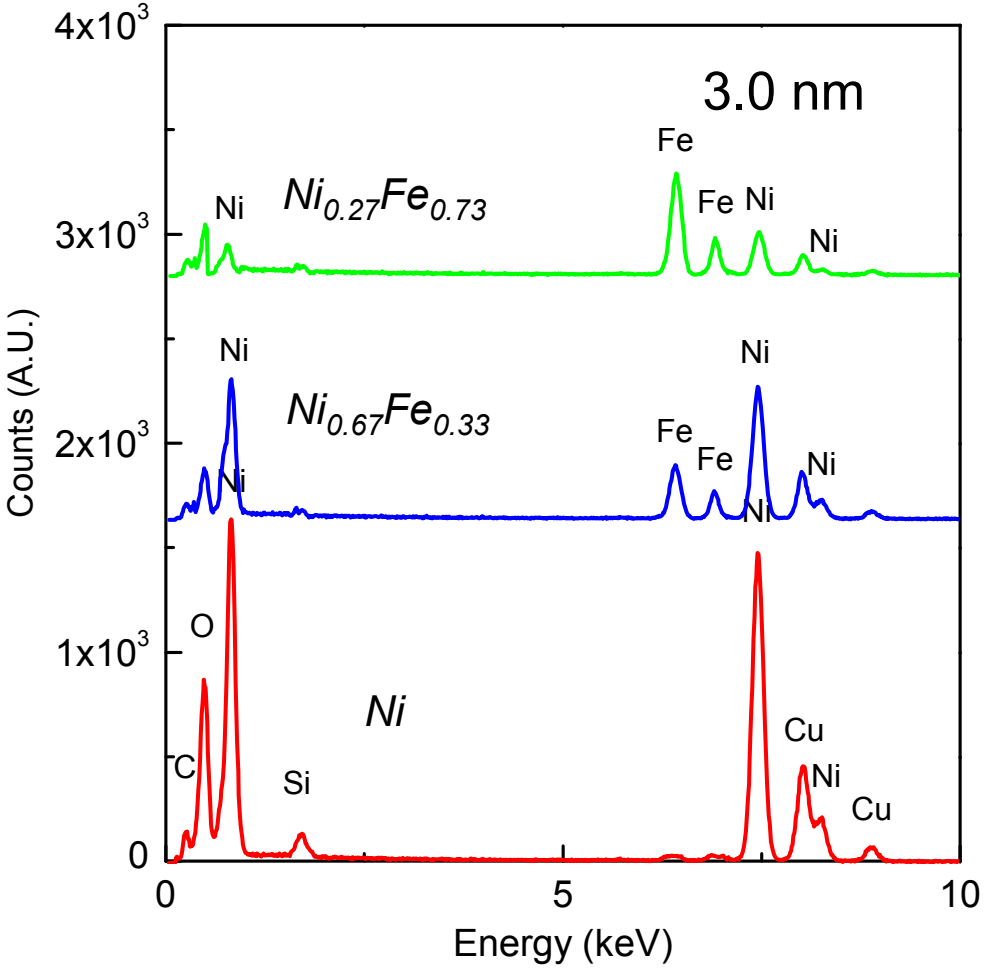

XRD of as-grown Ni_xFe_{1-x} bimetallic nanoparticles

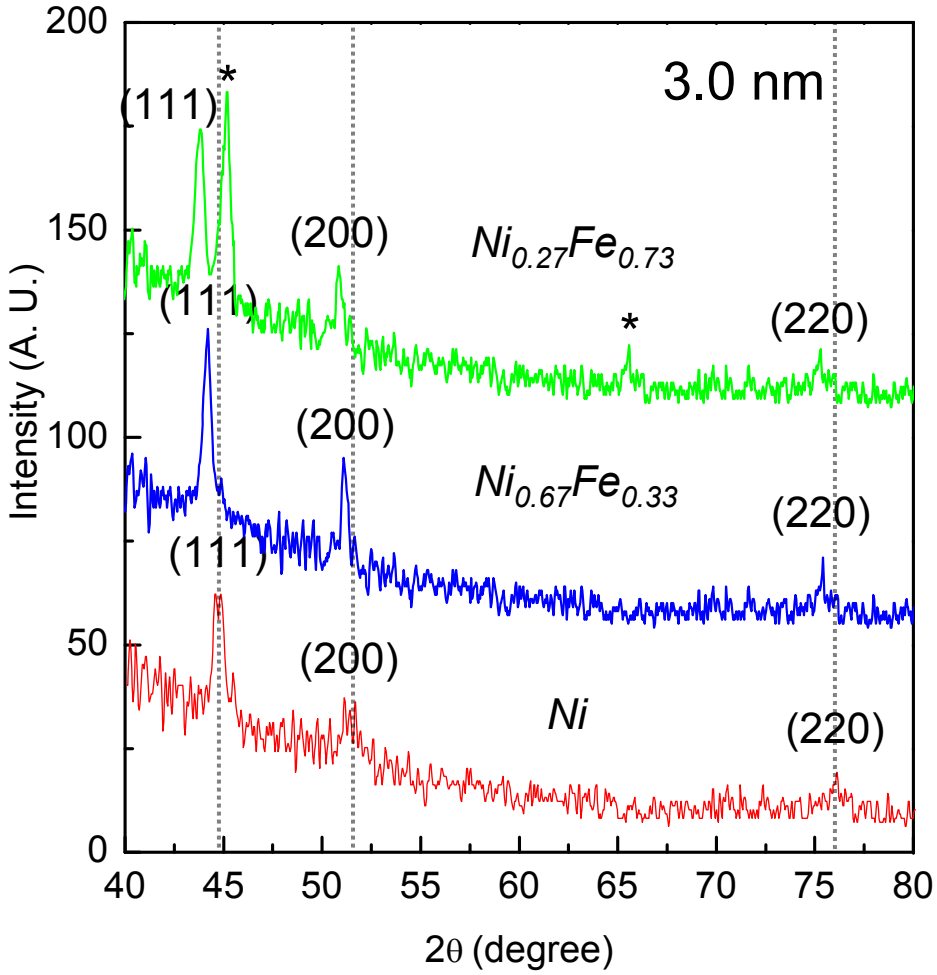

A priori design and synthesis of dimensionally- and compositionally-tuned bimetallic nanoparticles

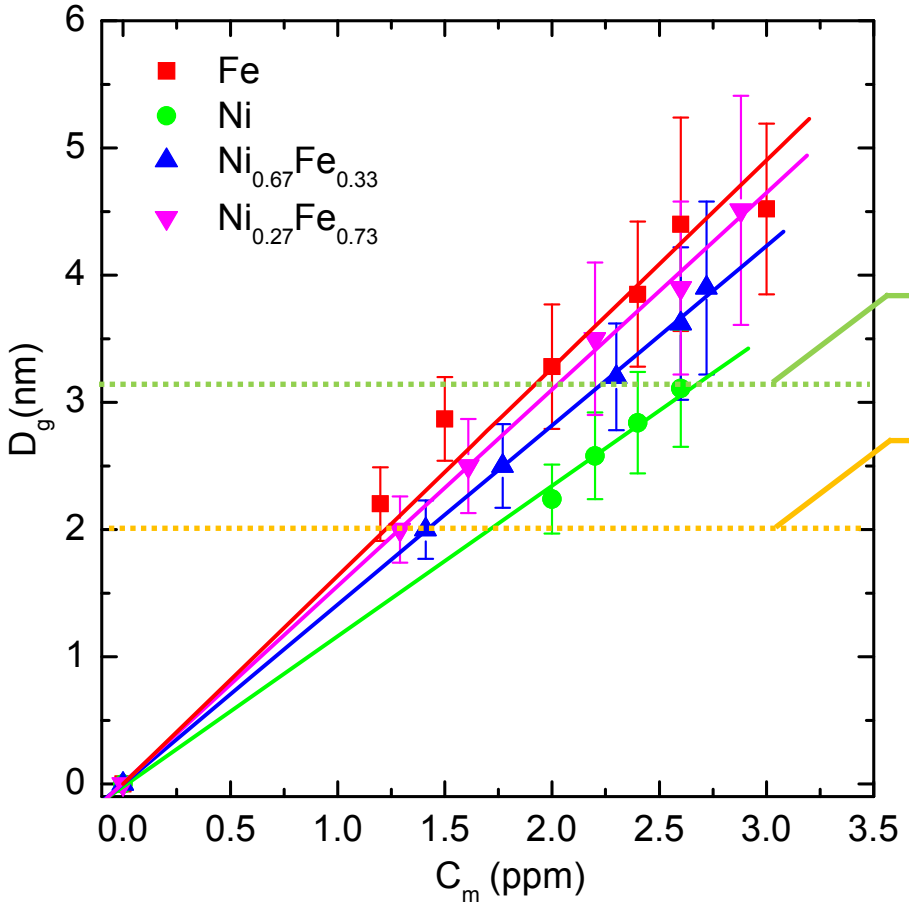

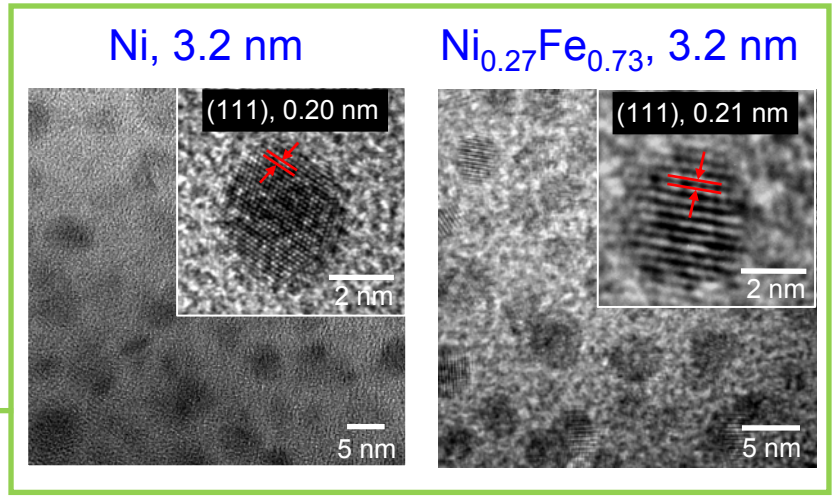

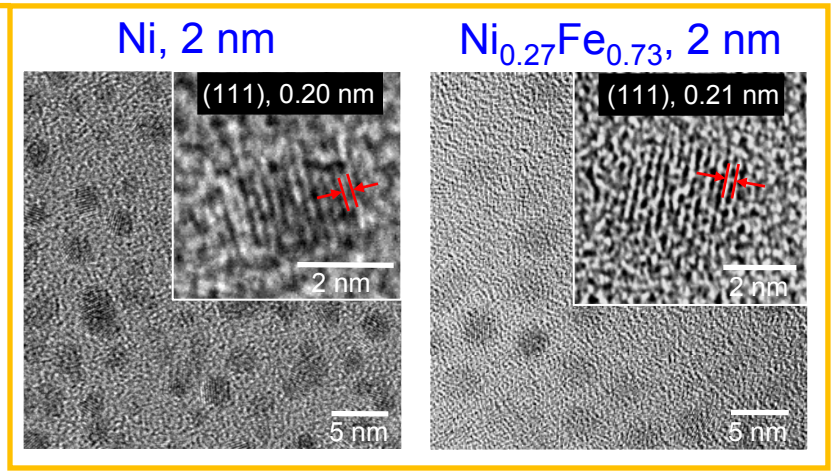

Catalytic growth of carbon nanotubes

Conventional approaches to catalyst preparation for carbon nanotube growth

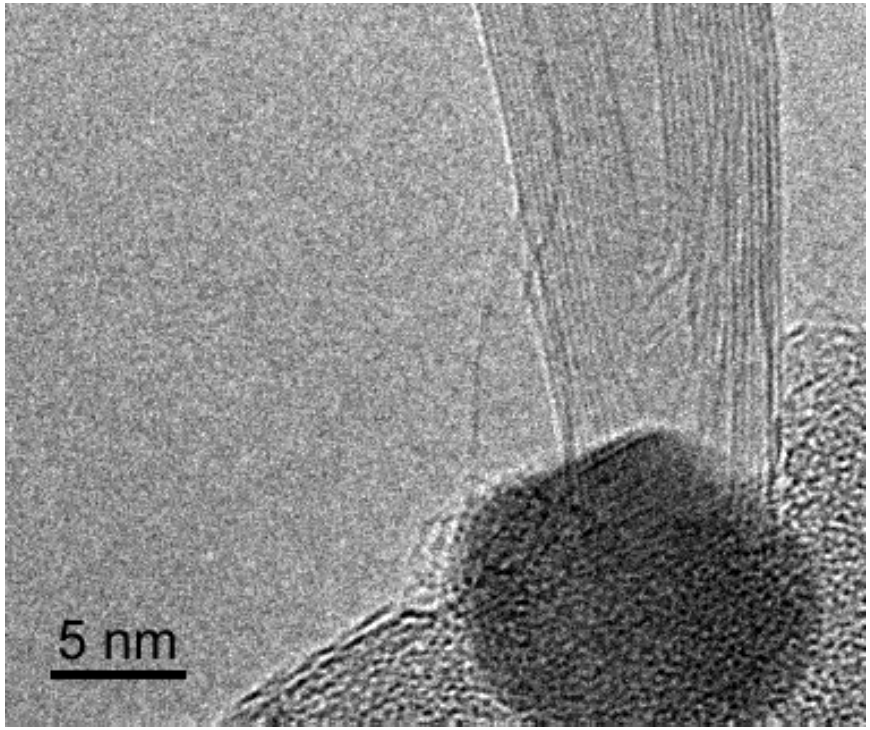

Yoshida *et al.*, Nano Lett., Vol. 8, 2082 (2008)

1. Floating catalyst method

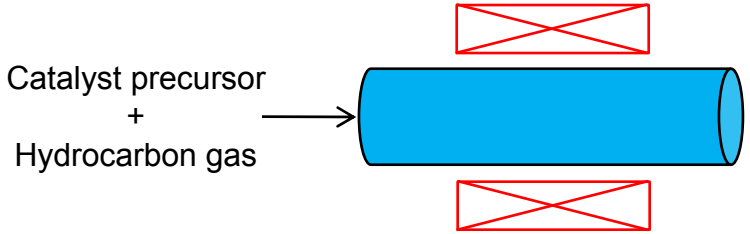

2. Substrate growth

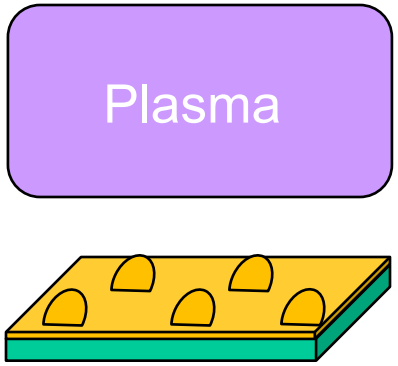

A new two step, sequential process for catalytic growth of CNTs

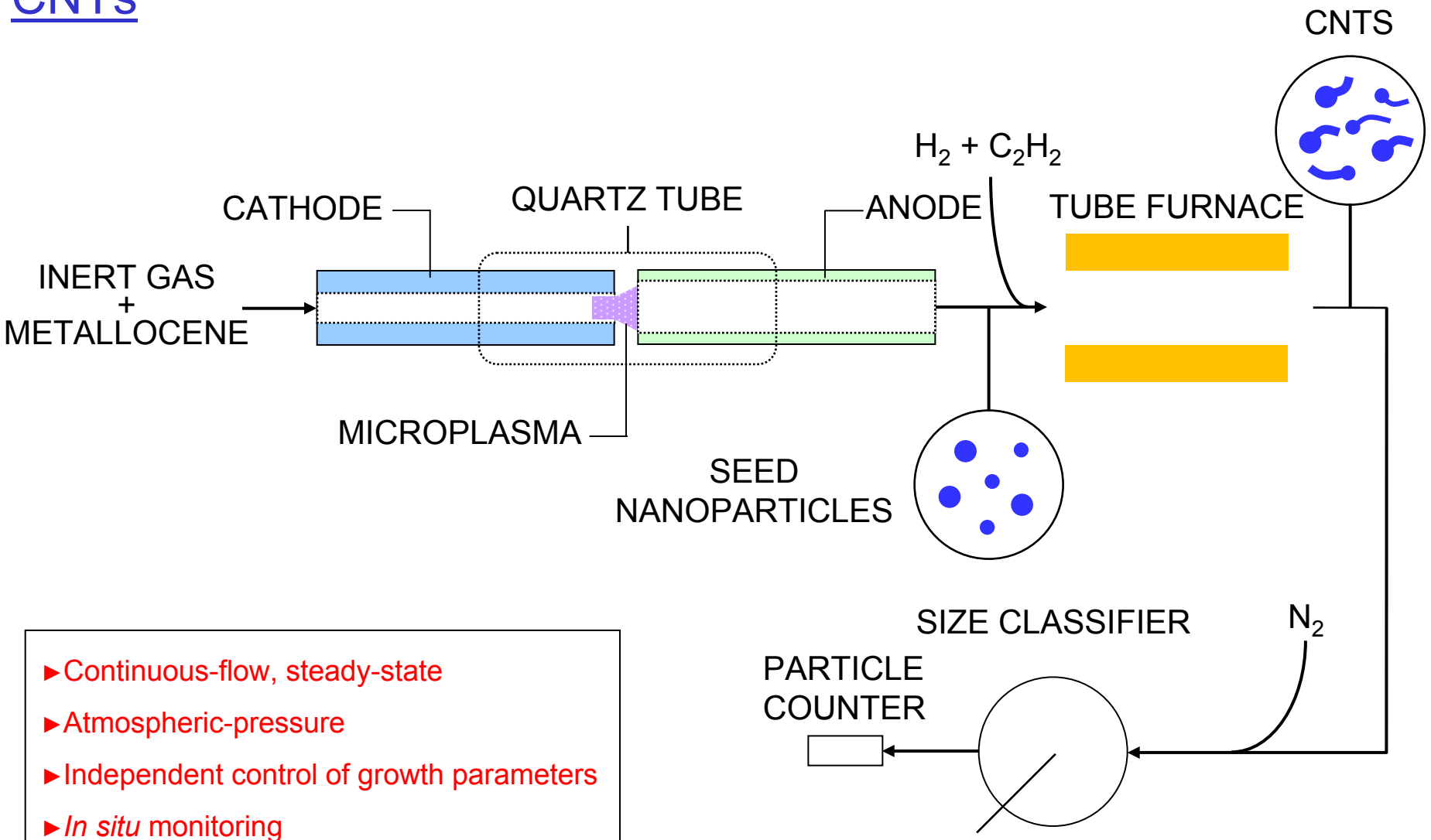

- ►Continuous-flow, steady-state
- ►Atmospheric-pressure
- ►Independent control of growth parameters
- ►*In situ* monitoring

Cylindrical differential mobility analyzer (TSI, Inc.)

Detects particles 2 nm < D_p < 100 nm

Aerosol monitoring of reactor effluent

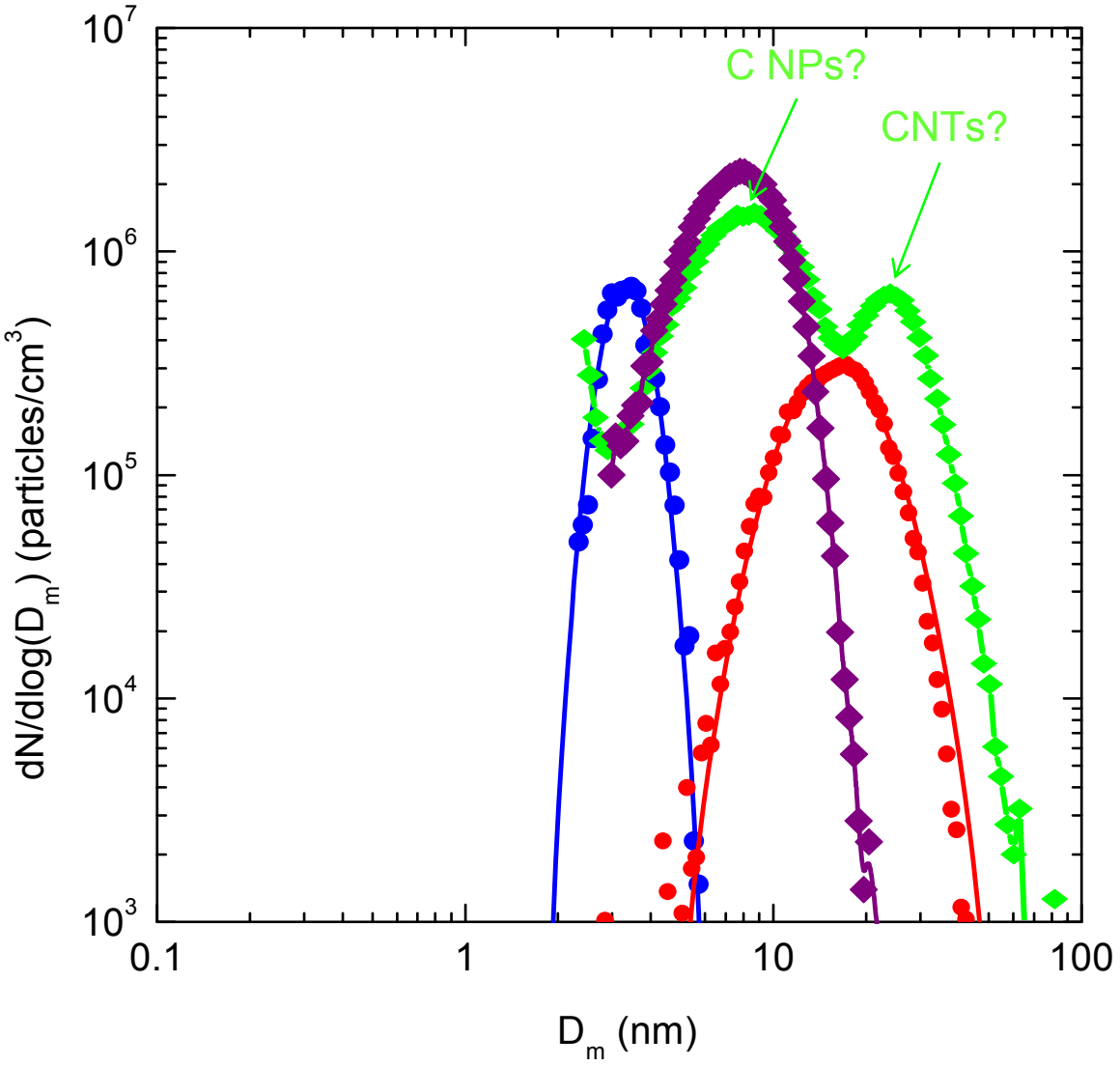

- Ni NPs room temp.
- 500 °C → CNTs?
- 700 °C → CNTs, C NPs?
- 700 °C + no catalyst → C NPs

<700 °C → only catalytic CNT growth!

Diameter-controlled growth of CNTs – Towards high-purity synthesis of SWCNTs

Ni 3.1 nm / MWCNTs

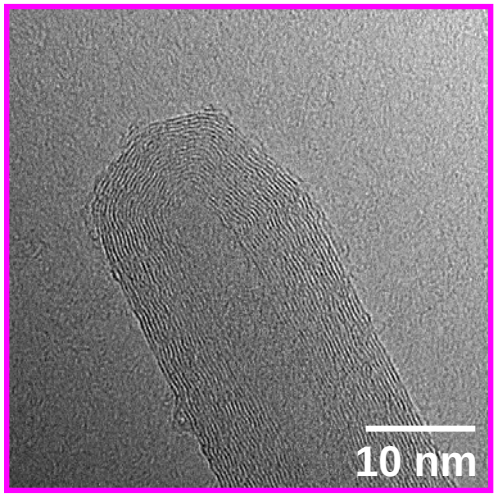

Ni 2.2 nm / SWCNTs

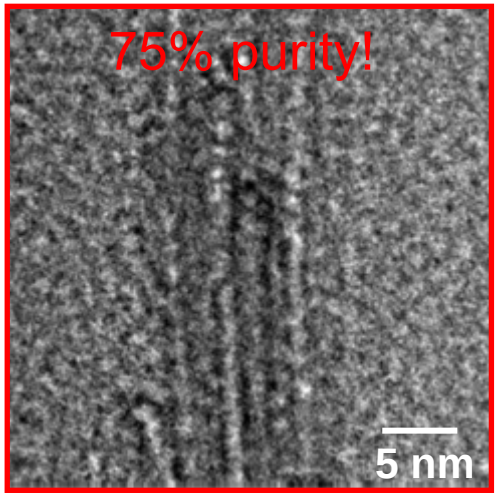

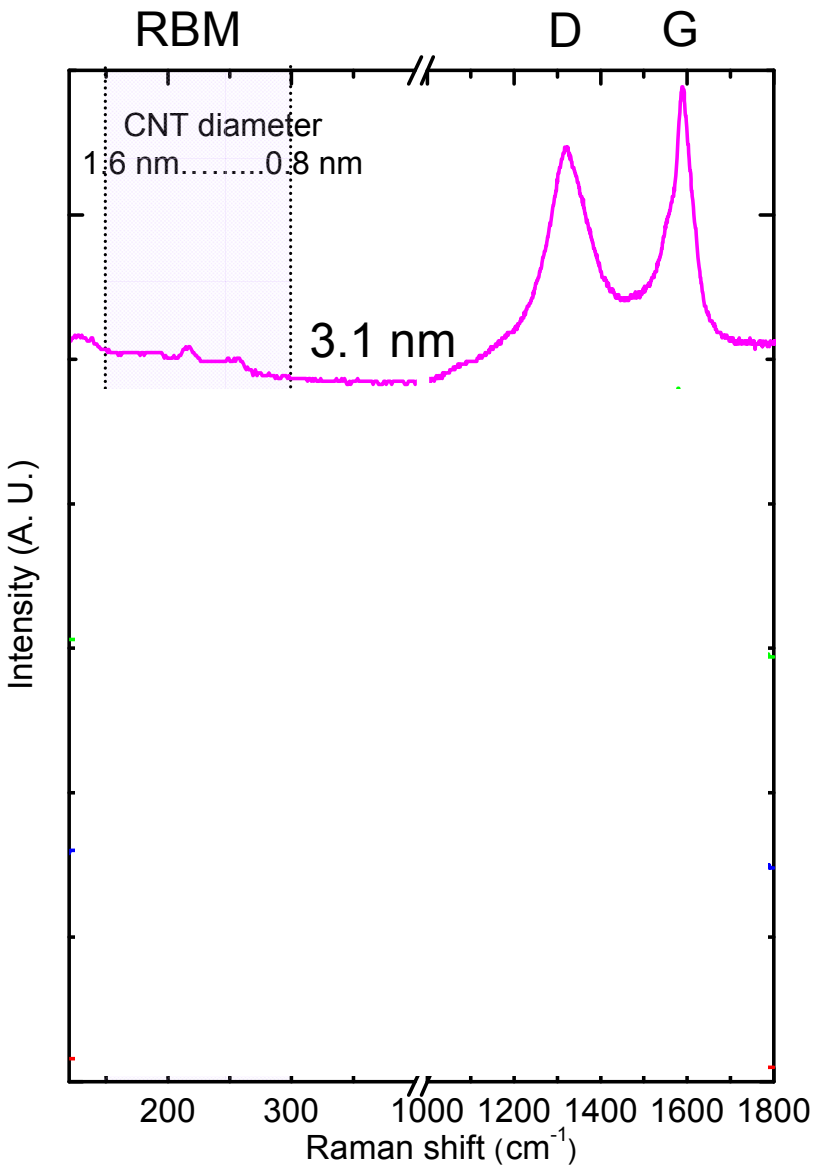

Ni 2.6 nm / TWCNTs

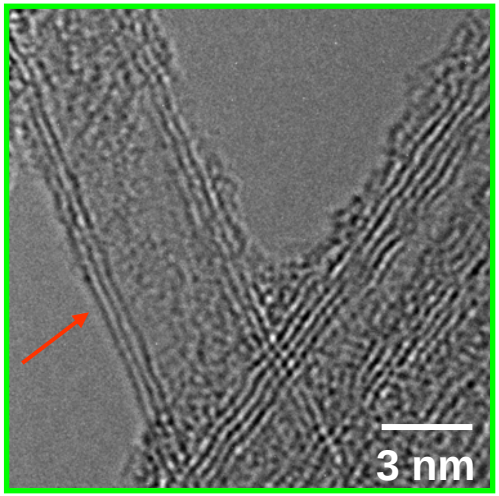

Ni 2.5 nm / DWCNTs

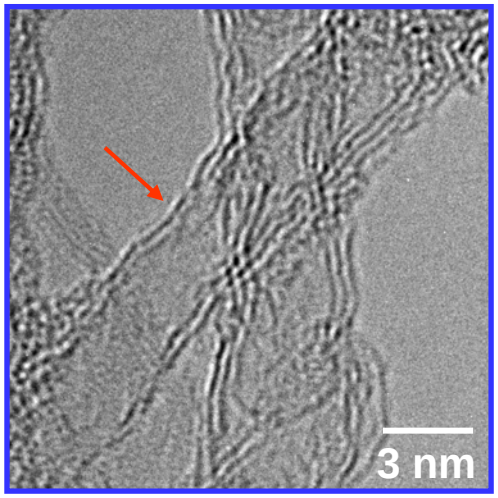

(n,m) chirality / structure of SWCNTs (electronic type)

metallic (m): n-m=3i
semiconducting (s): n-m≠3i

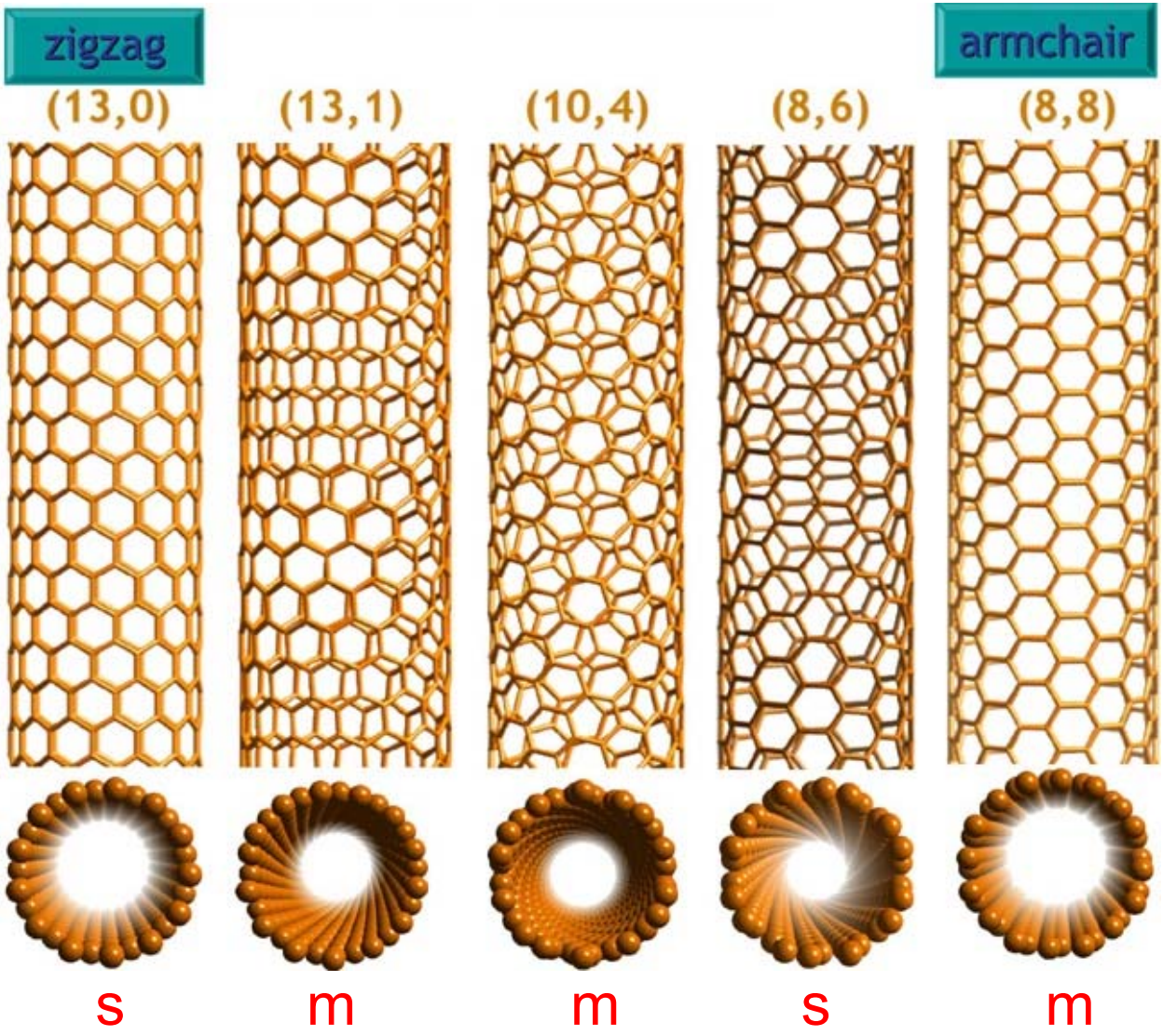

Collecting and dispersing SWCNTs for optical characterization

Glassy fiber filter

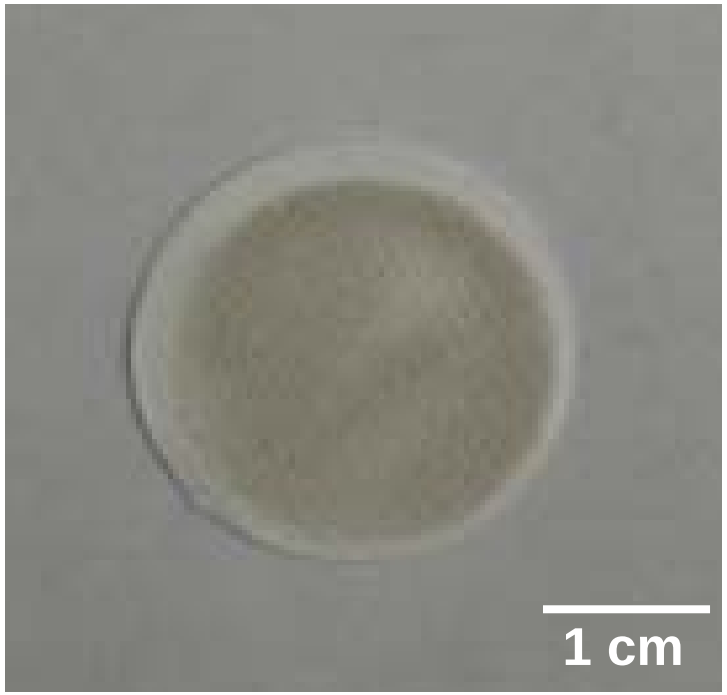

Sonication (24 hrs)
+
Ultracentrifuging
(38000g, 2 hrs)

SWCNT dispersion

- 0.17 mg/hr (no purification) (for single microplasma reactor)

- Sodium dodecyl sulfate (SDS) + D_2O

UV-Vis-NIR absorbance: *Effect of catalyst size*

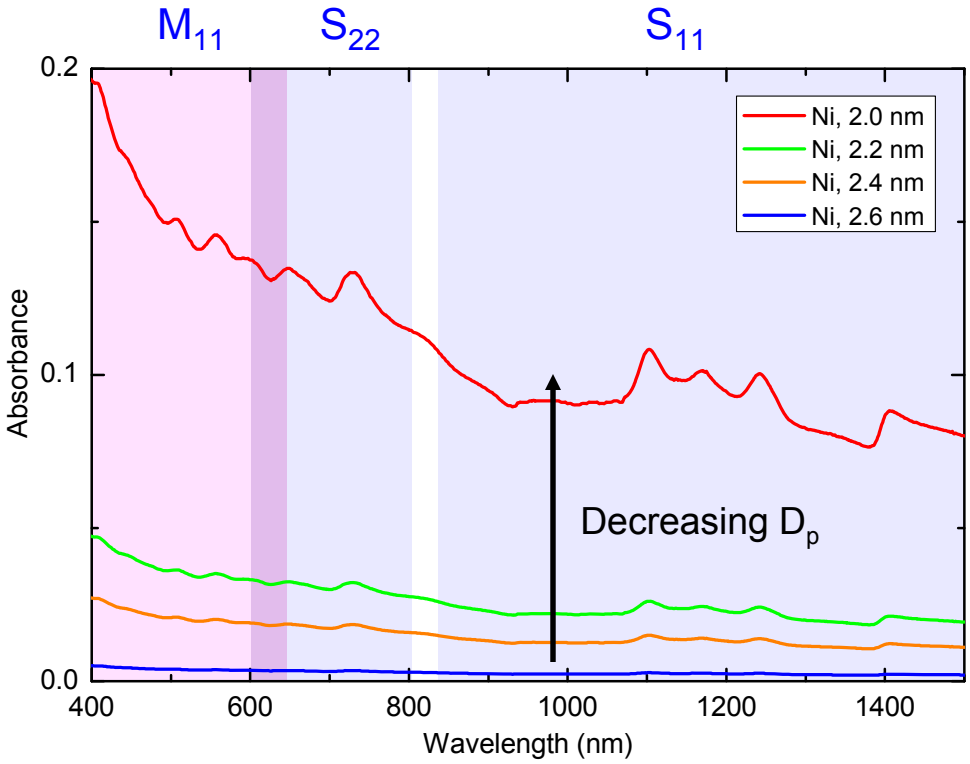

- Overall yield (absorbance) of SWCNTs decreases with increasing particle size

UV-Vis-NIR: *Effect of catalyst composition*

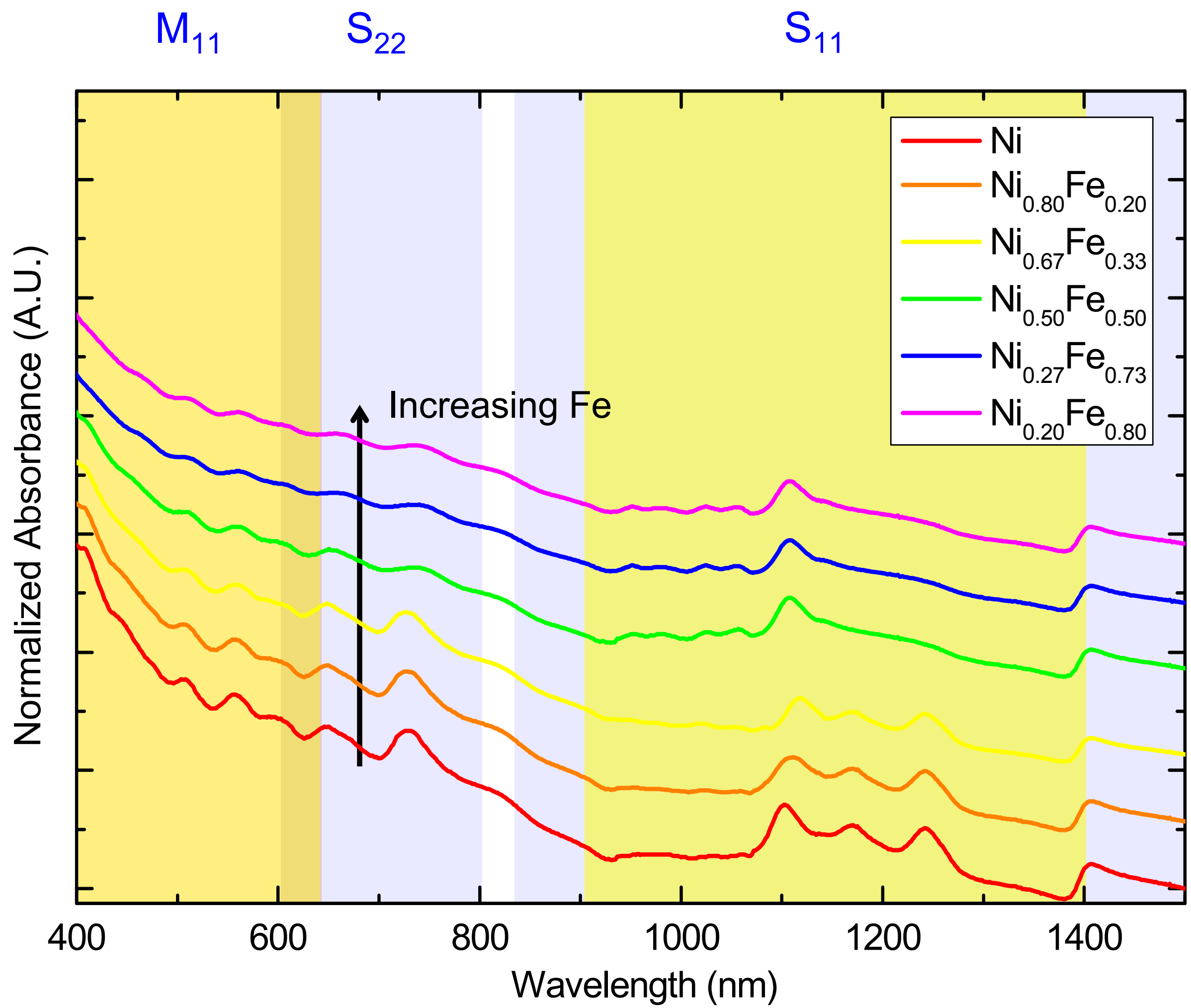

Significant changes in semiconducting population distribution as the nanocatalyst composition is varied

Lower metallic content in nanotubes catalyzed by nanoparticles with higher Fe at%

Photoluminescence spectroscopy of SWCNTs

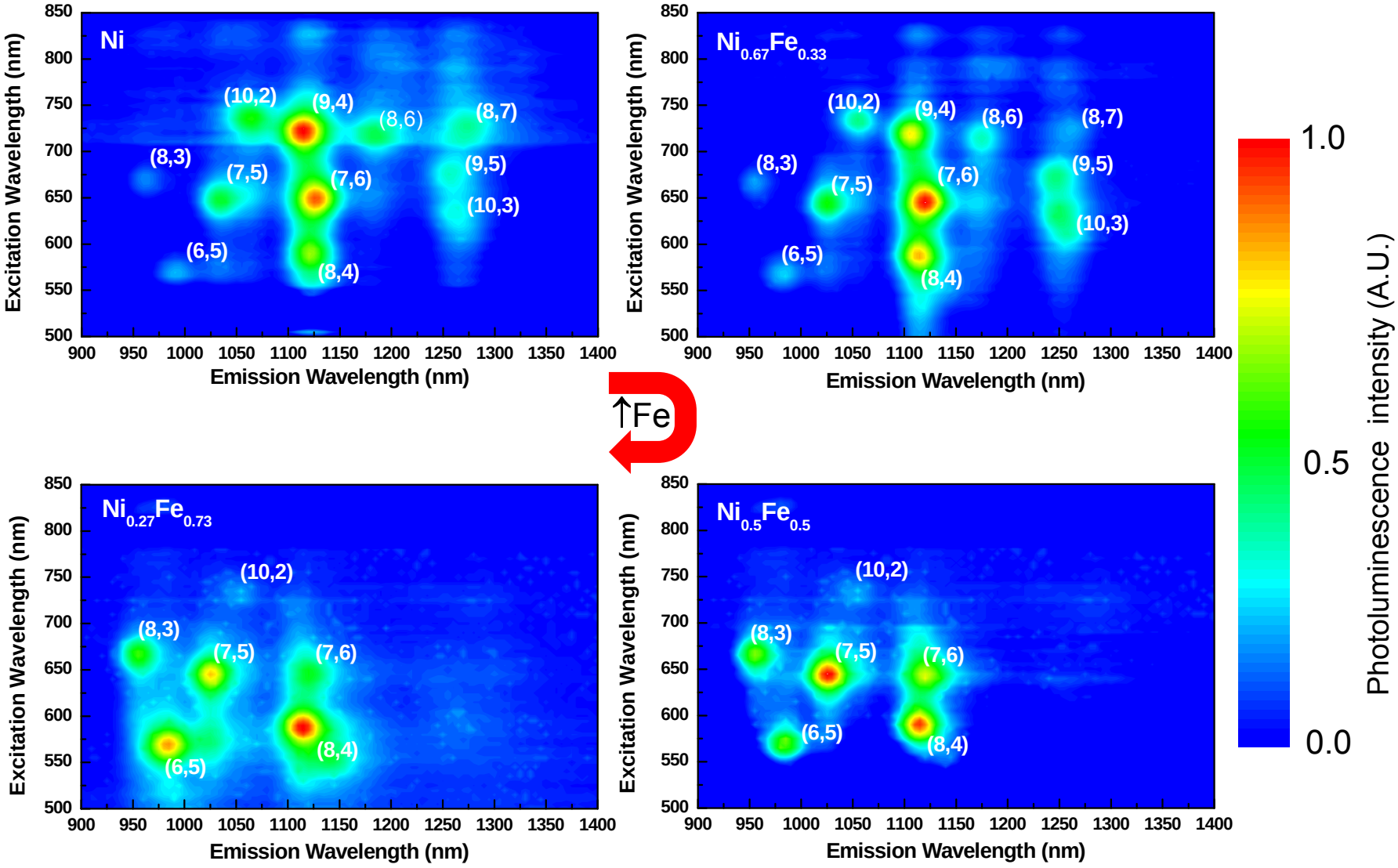

Relative abundance of different semiconducting chiralities changes with nanocatalyst composition

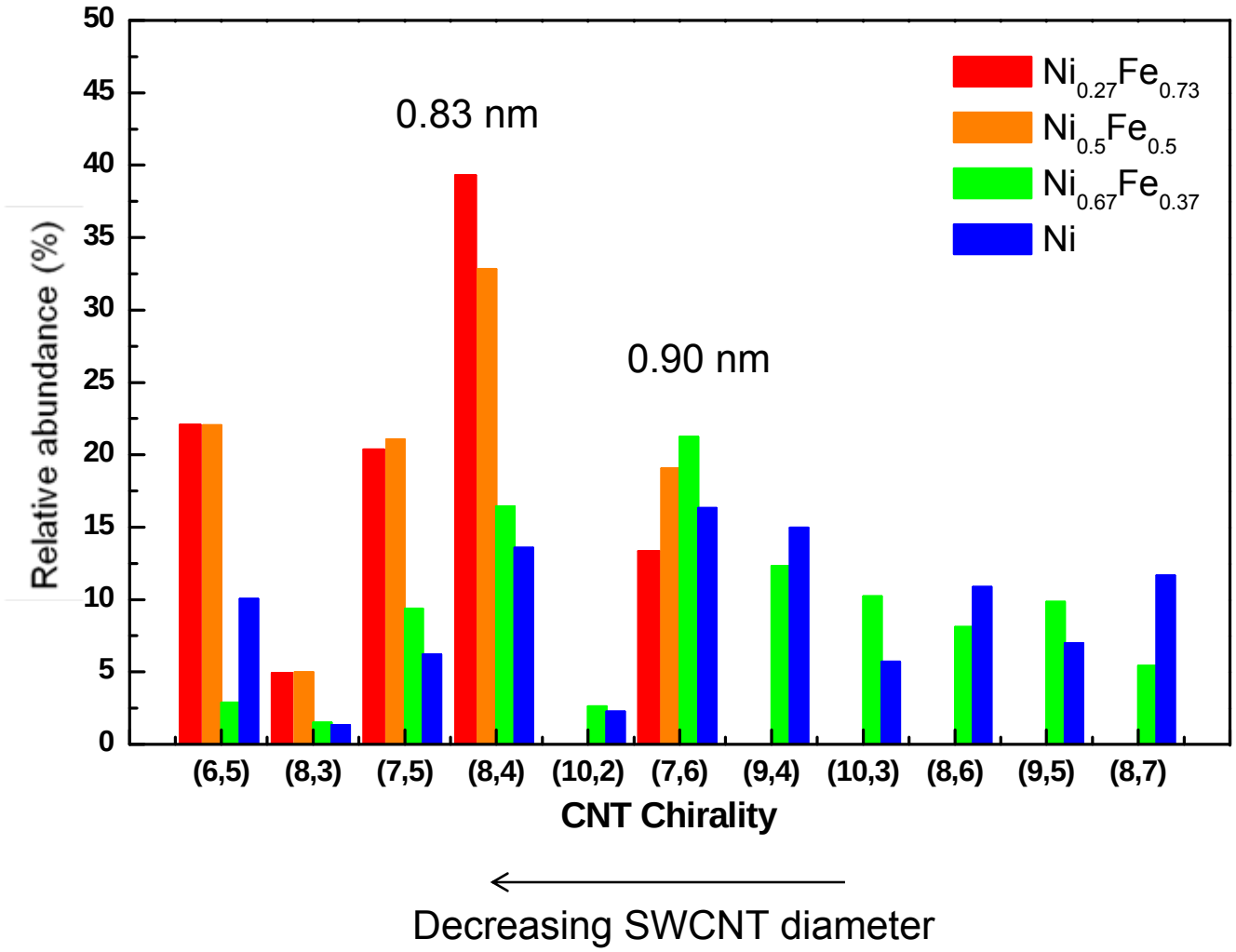

Model for SWCNT growth based on lattice matching (epitaxial growth)

Ni(111) bond length: 0.249 nm
Graphene lattice constant: 0.248 nm

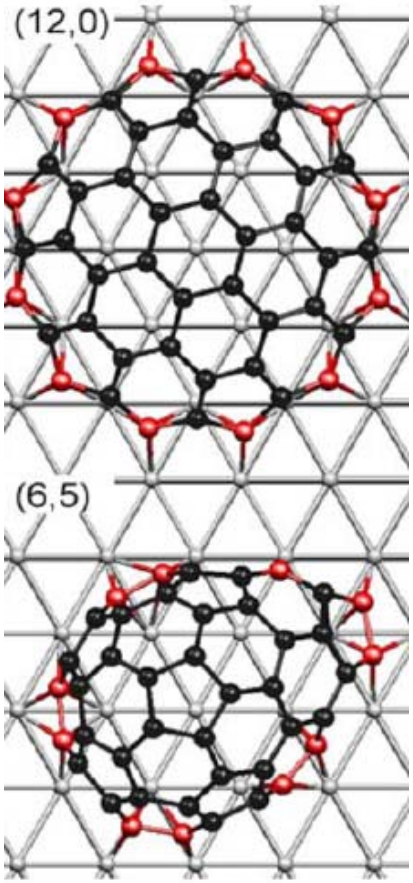

S. Reich *et al.*, Chem. Phys. Lett., Vol. 421, 469 (2006)

Multi line excitation micro Raman spectroscopy of SWCNTs

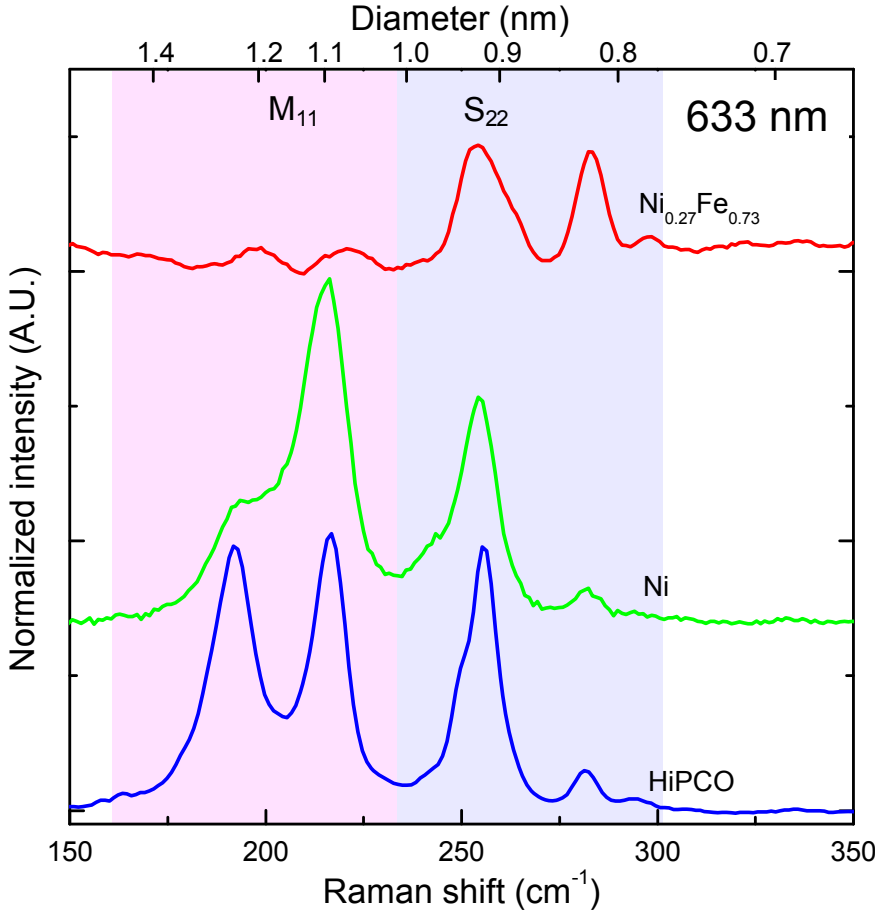

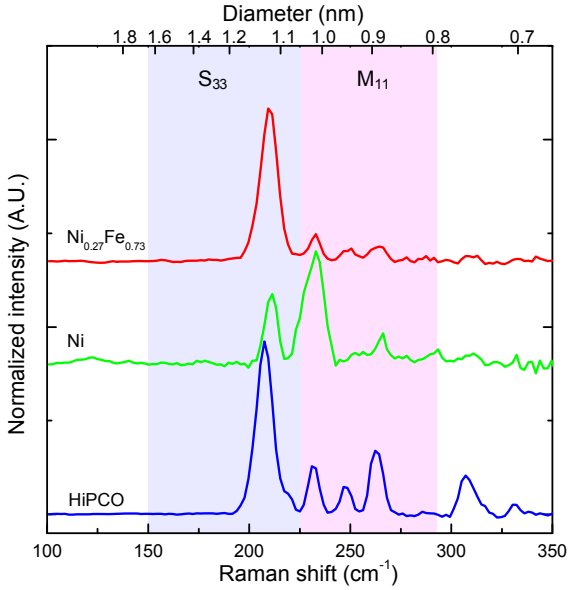

488 nm

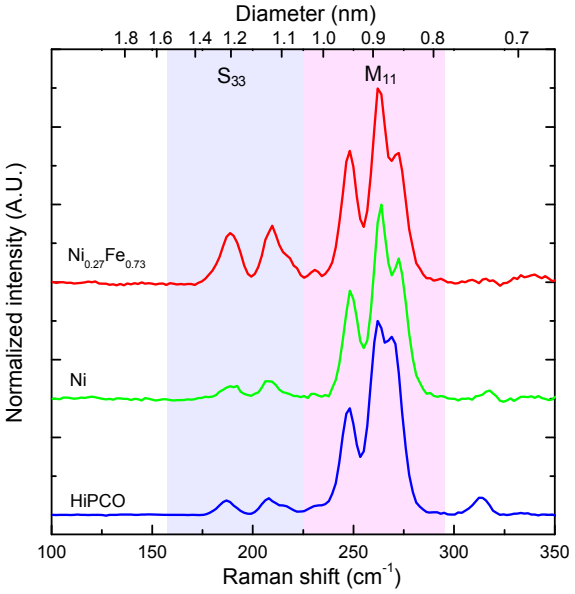

514 nm

Relative amount of semiconducting and metallic nanotubes changes with catalyst composition

Excitation wavelength (nm)	Temperature (°C)	Catalyst	% semiconducting	% metallic	FWHM of G-band intensity (cm^{-1})
633		HiPCO	62.9	37.1	--
	600	Ni	66.8	33.2	--
	600	$Ni_{0.27}Fe_{0.73}$	90.5	9.5	--
	700	$Ni_{0.27}Fe_{0.73}$	55.5	44.5	--
488		HiPCO	62.9	37.1	--
	600	Ni	63.4	36.6	--
	600	$Ni_{0.27}Fe_{0.73}$	85.5	14.5	--
514		HiPCO	62.9	37.1	40
	600	Ni	60.2	39.8	39
	600	$Ni_{0.27}Fe_{0.73}$	84.2	15.8	25

Fabrication of thin film SWCNT-based FETs

Schematic of single device:

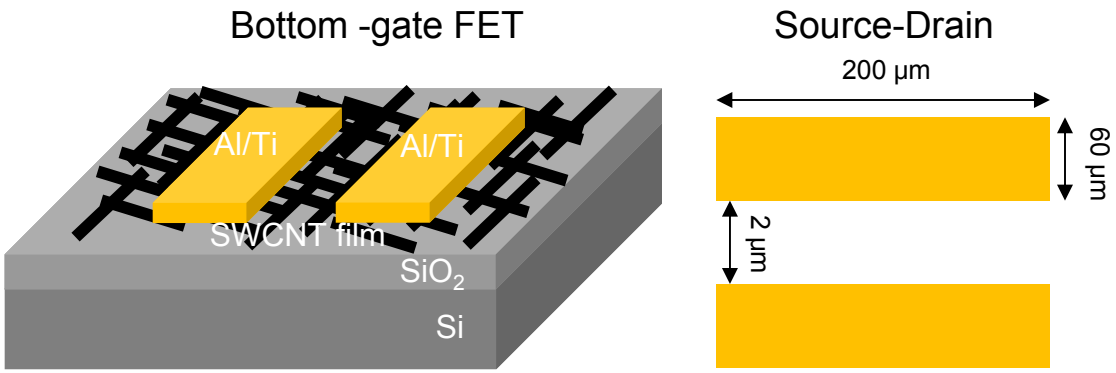

SEM of multiple devices fabricated in parallel:

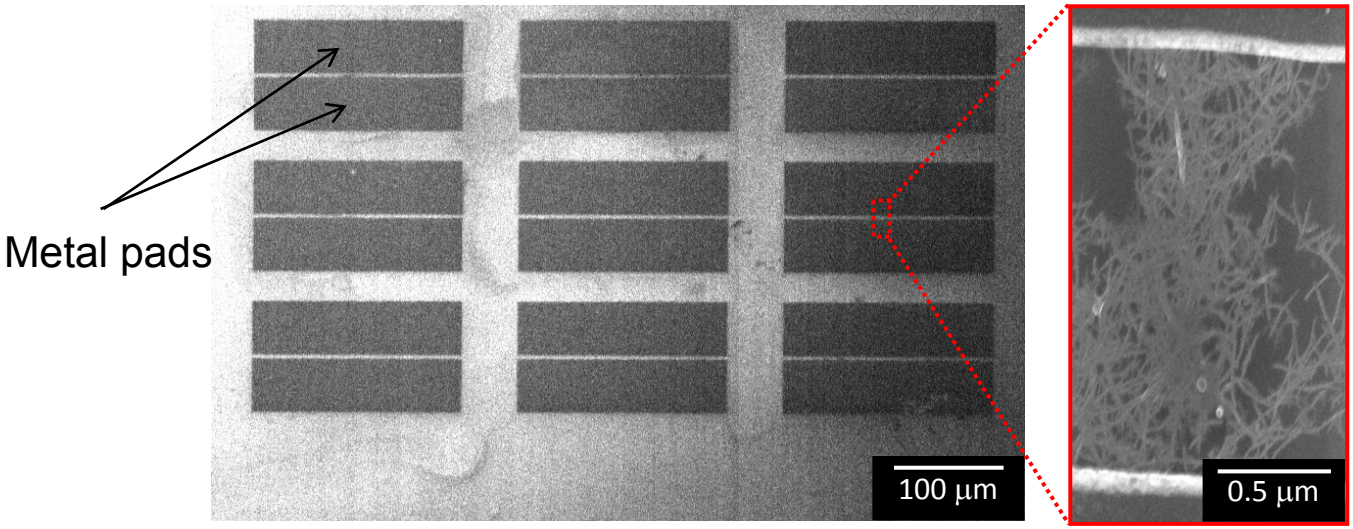

Electrical characterization of SWCNT-based FETs

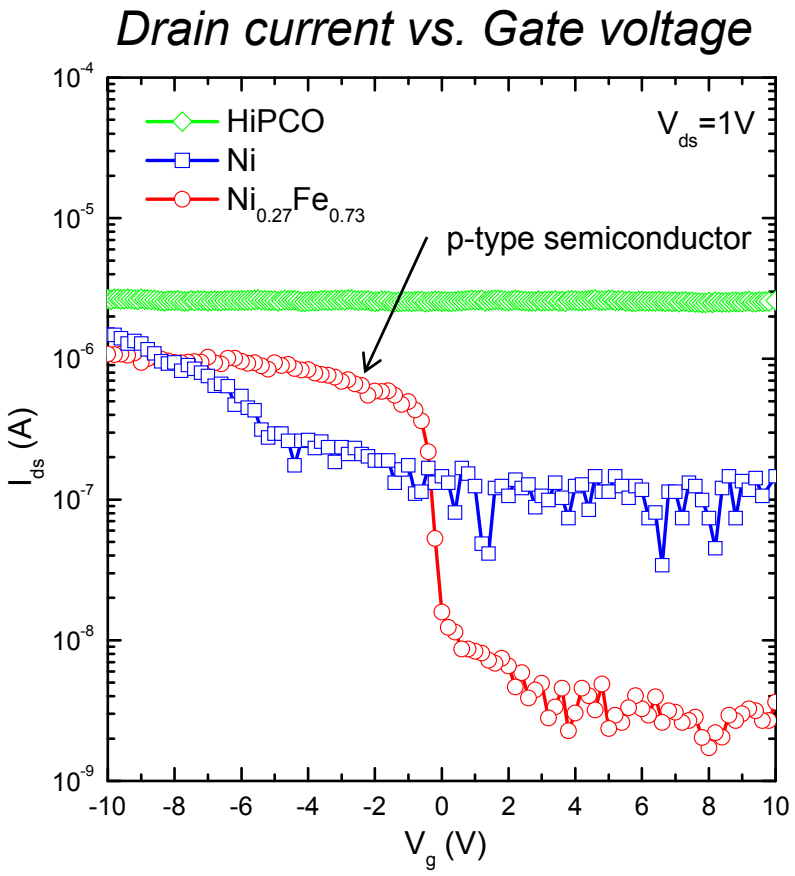

Plasma-liquid electrochemistry

A hybrid microplasma-based electrochemical cell

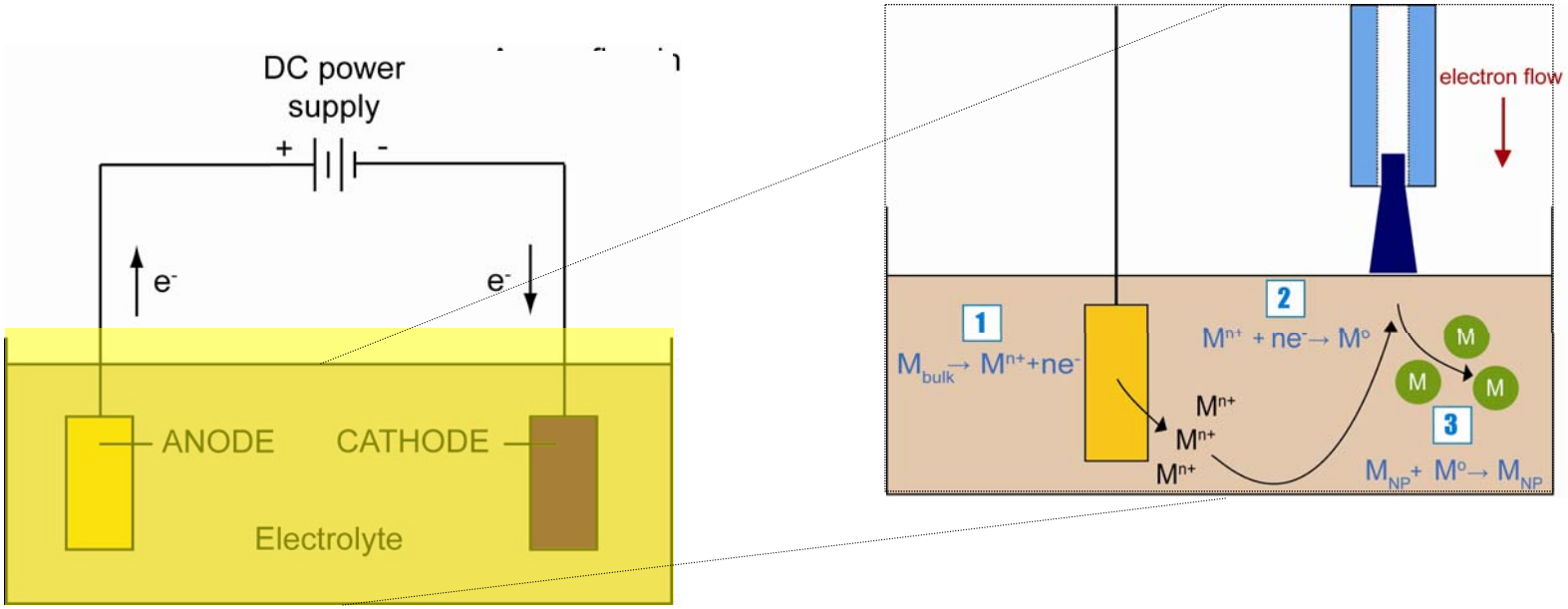

1. Anodic dissolution of metal foil
2. Reduction of metal ions at microplasma
3. Nucleation, growth, and capping of particles

Microplasma-assisted electrochemical synthesis of colliodal Ag nanoparticles from bulk precursor

t=5 min

t=7 min

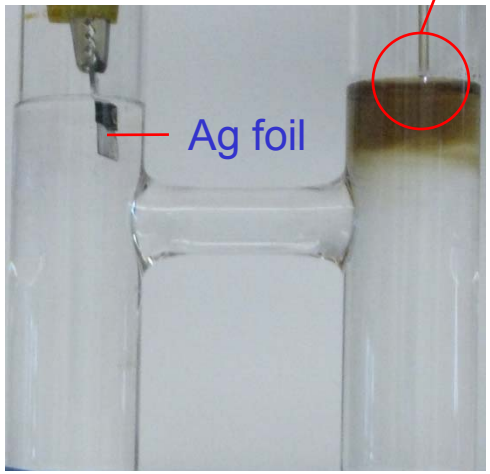

t=9 min

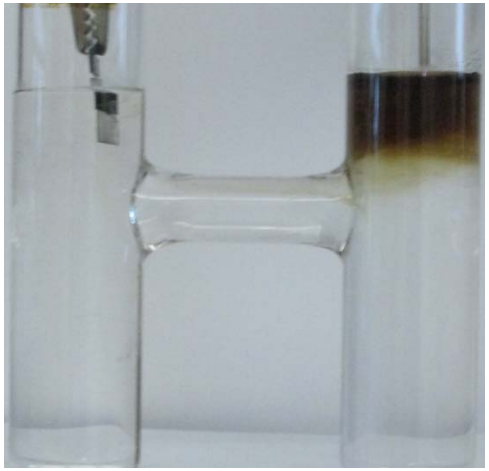

- ►Atmospheric-pressure, near room temperature
- ►Gas conduit for current flow (contact-less)
- ►Rapid reduction of aqueous metal cations
- ►Versatile (metal precursor, stabilizer molecule)

Efficiency of cell operated with microplasma

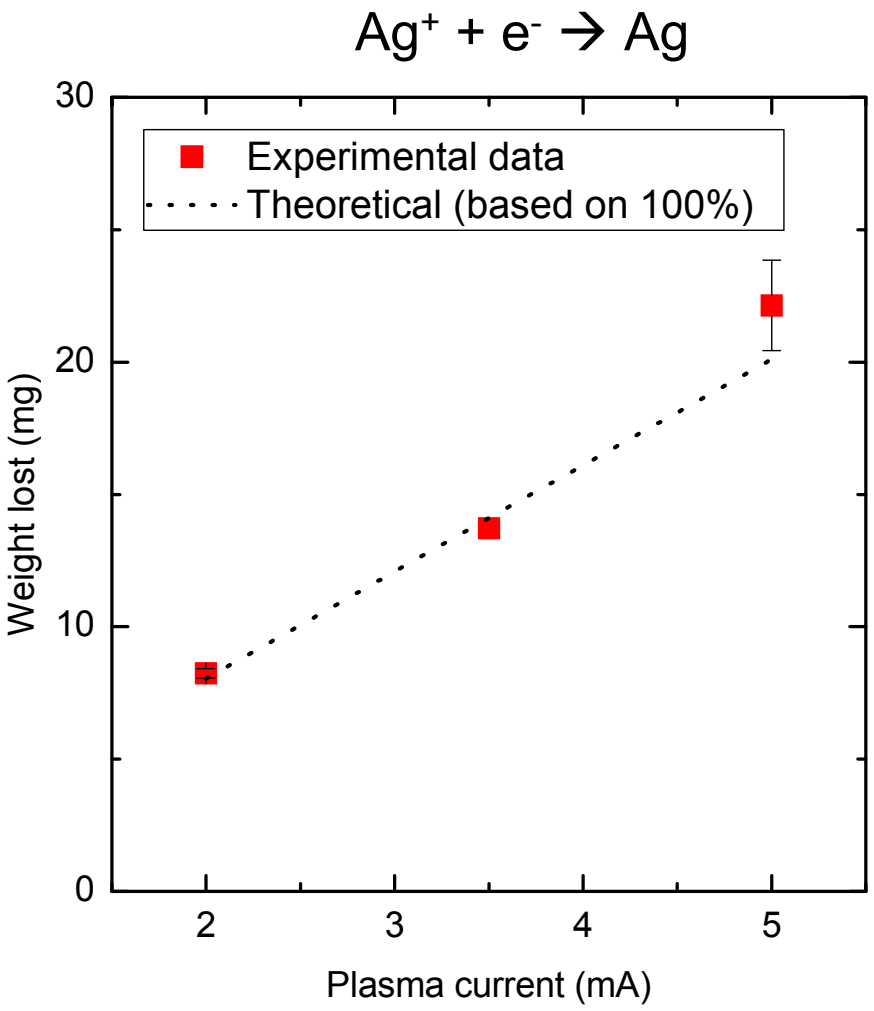

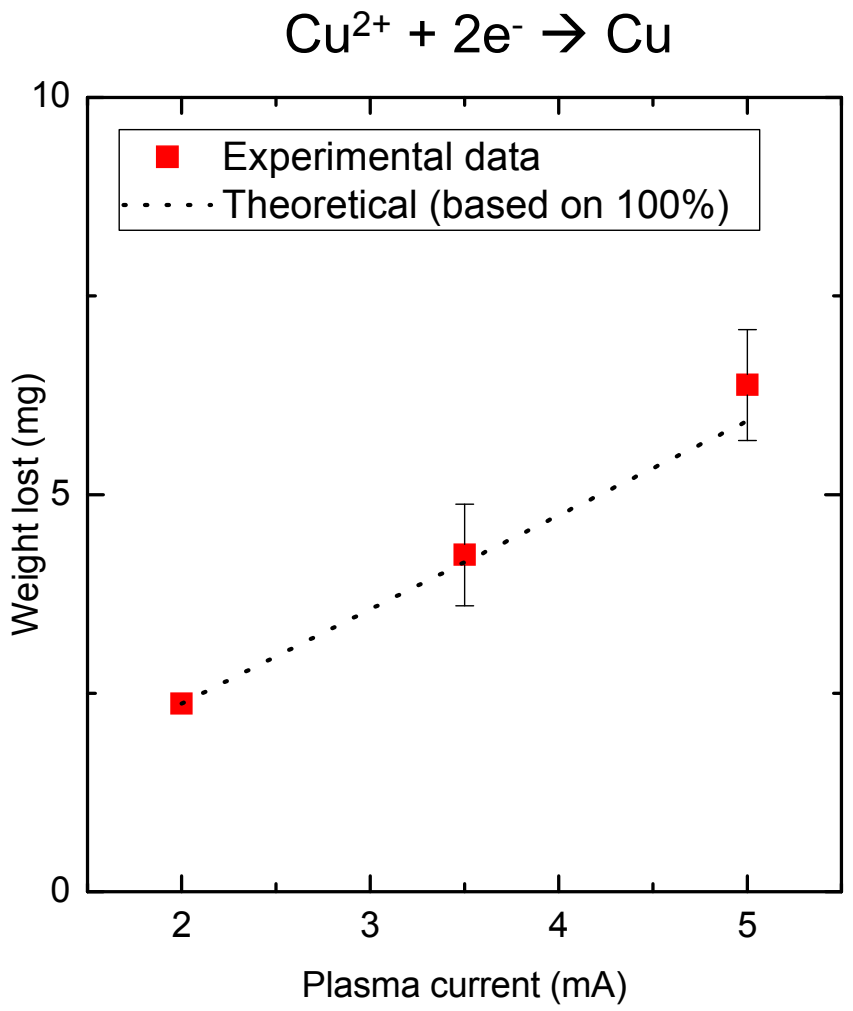

UV-visible absorbance of Ag and Au nanoparticle colloids

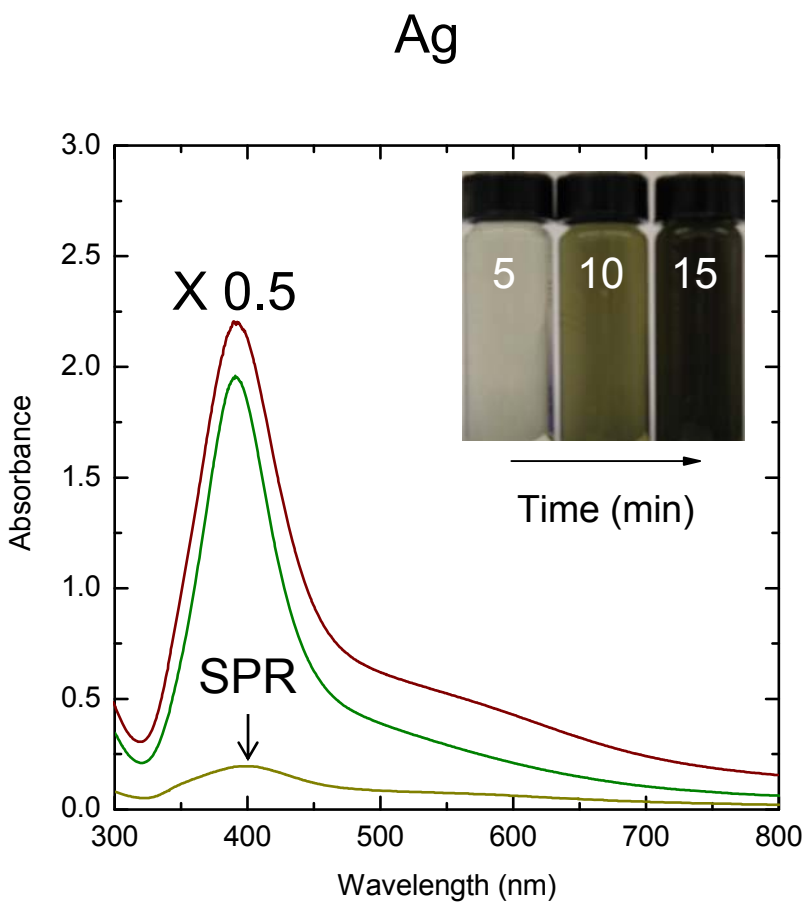

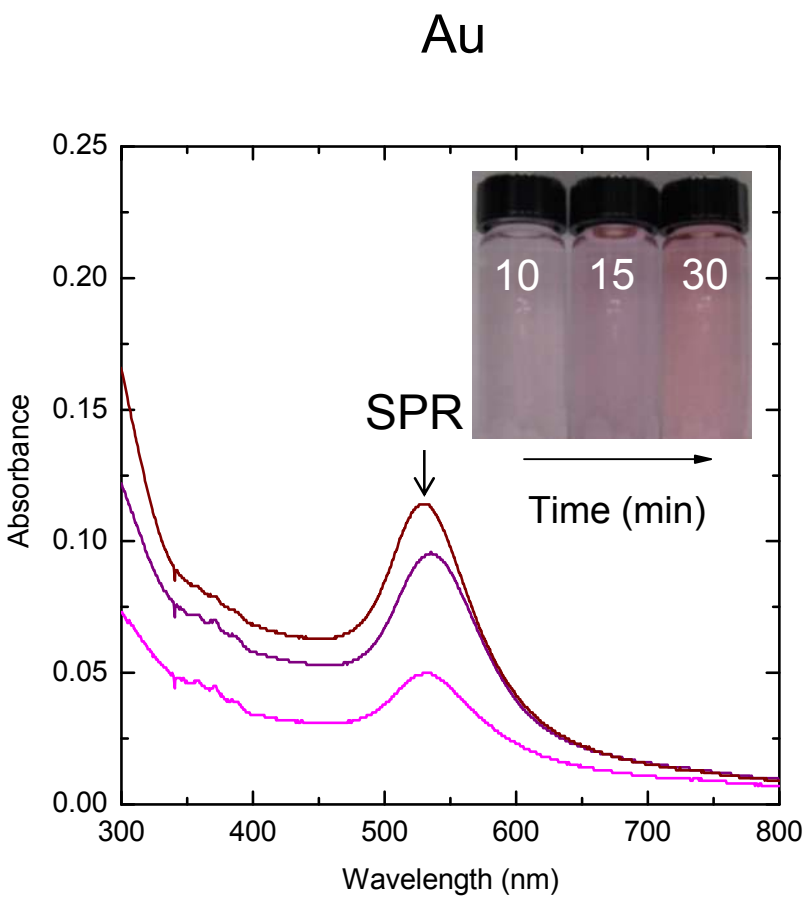

TEM of Ag and Au nanoparticles

Ag

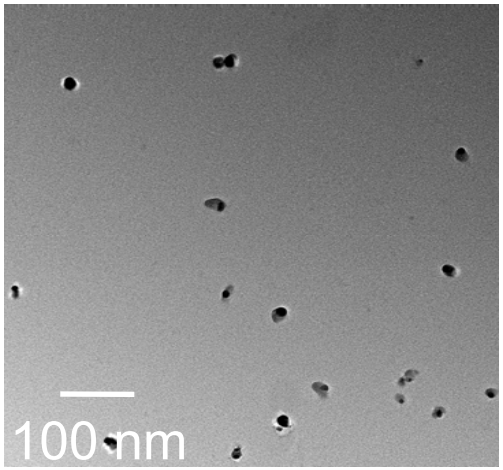

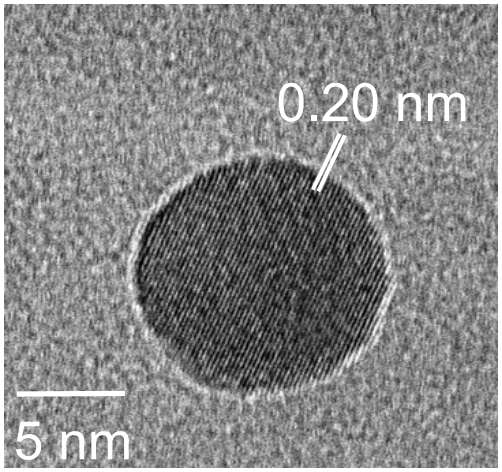

Au

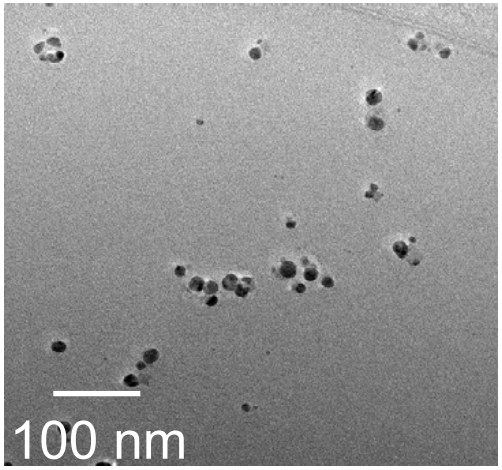

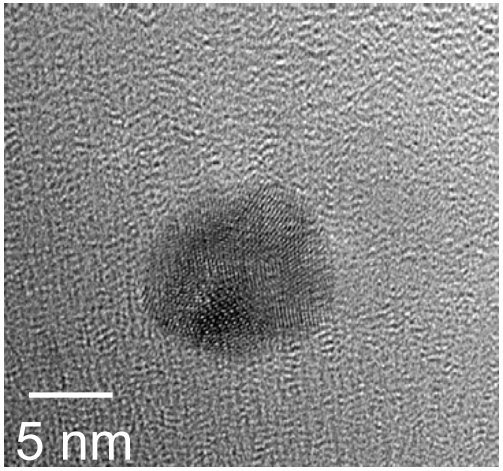

Microplasma reduction of metal salts – Pt anode/$HAuCl_4$

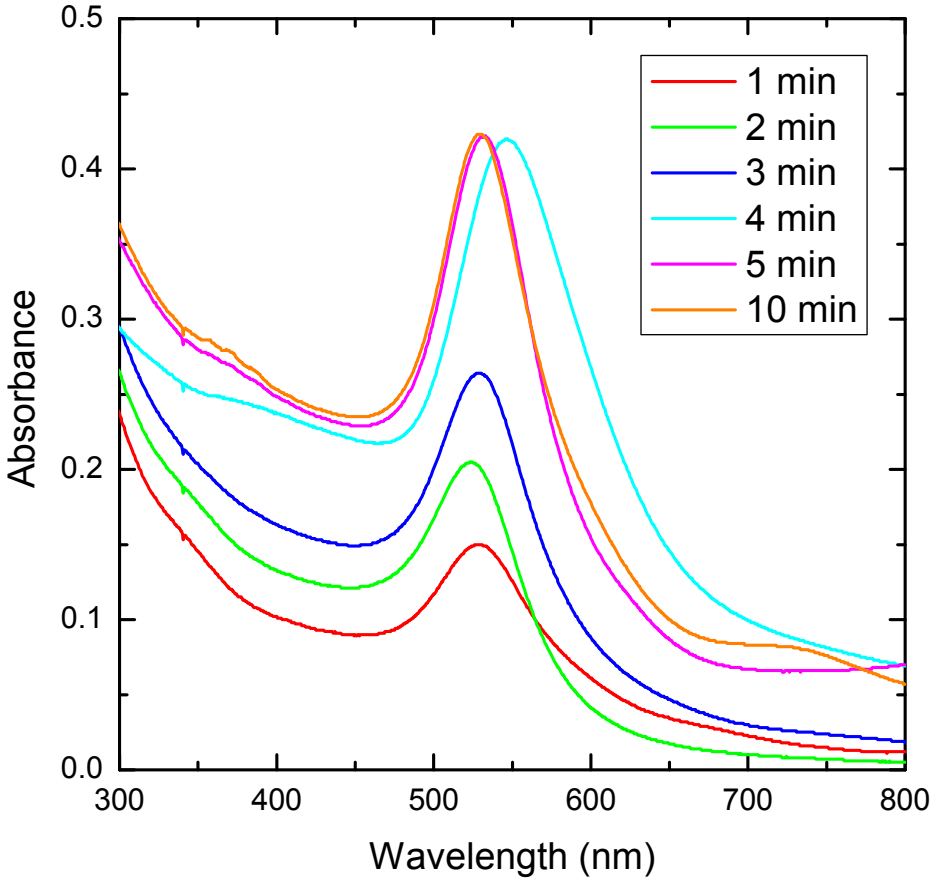

0.0001 M $HAuCl_4$ in water

Time (min)

Synthesis of Ag nanoparticle colloids for point-of-use SERS applications

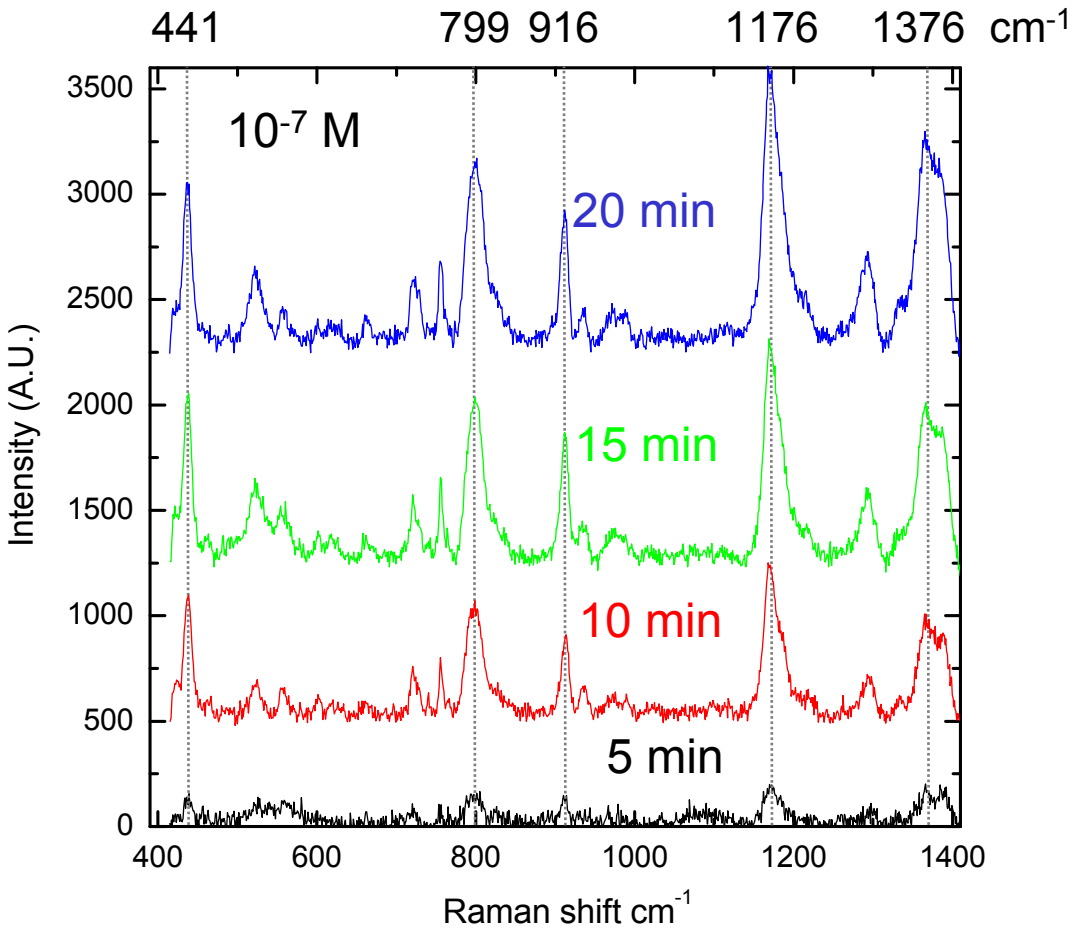

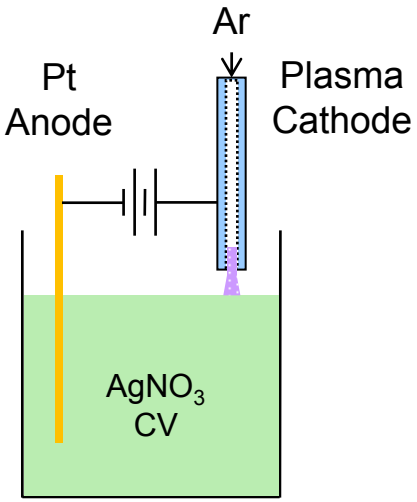

Crystal violet:

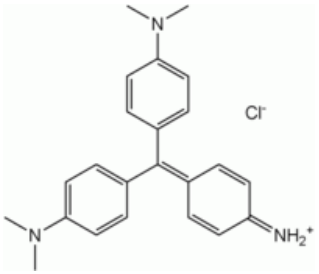

Non-lithographic fabrication of patterned nanoparticle films

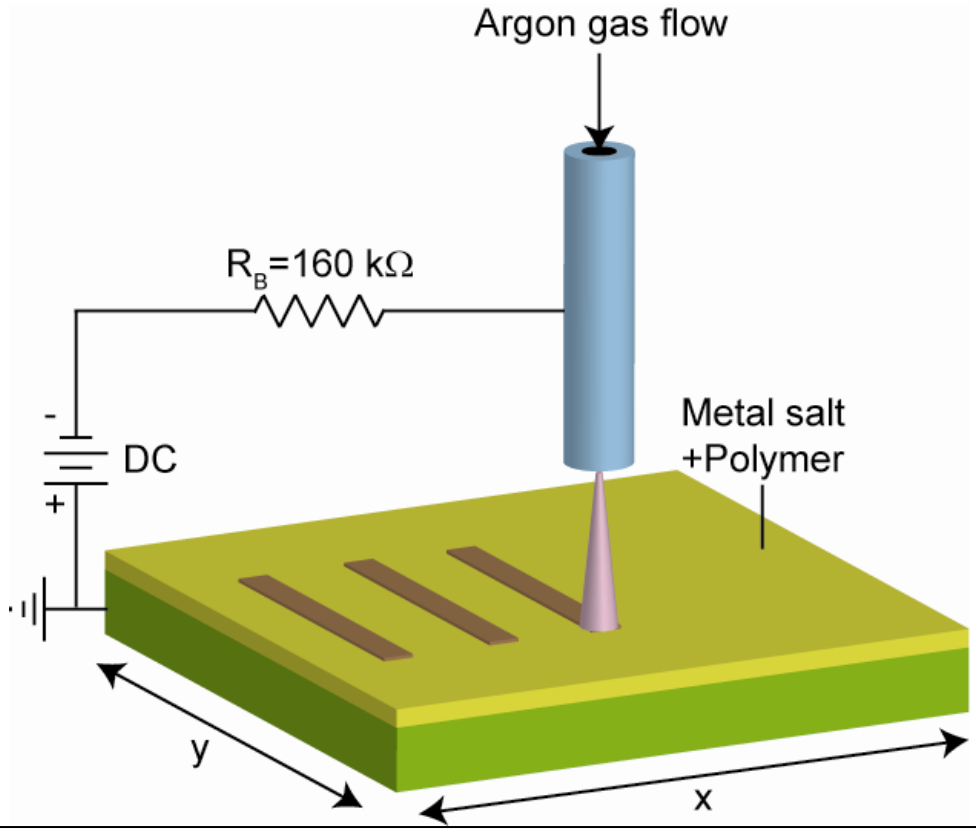

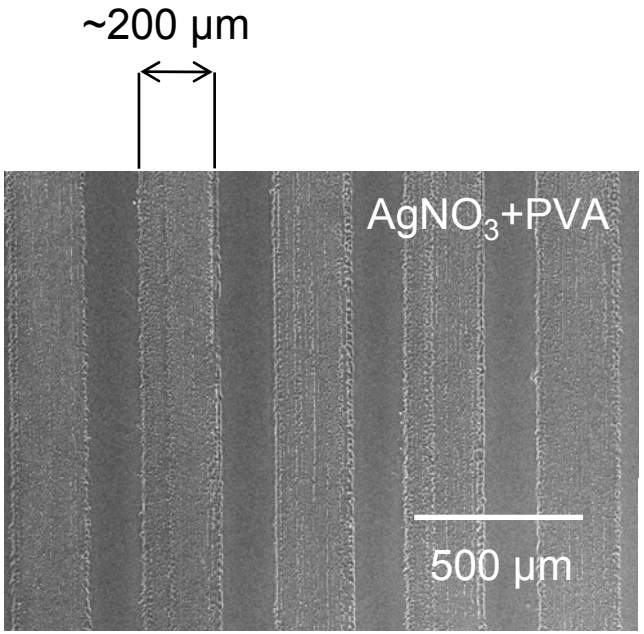

- ▸Atmospheric-pressure, near room temperature
- ▸~100 micron lateral resolution
- ▸Polymer and metal salt are interchangeable
- ▸Particle size depends on metal salt concentration

Reduction of wide range of metal salts is possible

XRD spectra of thin films:

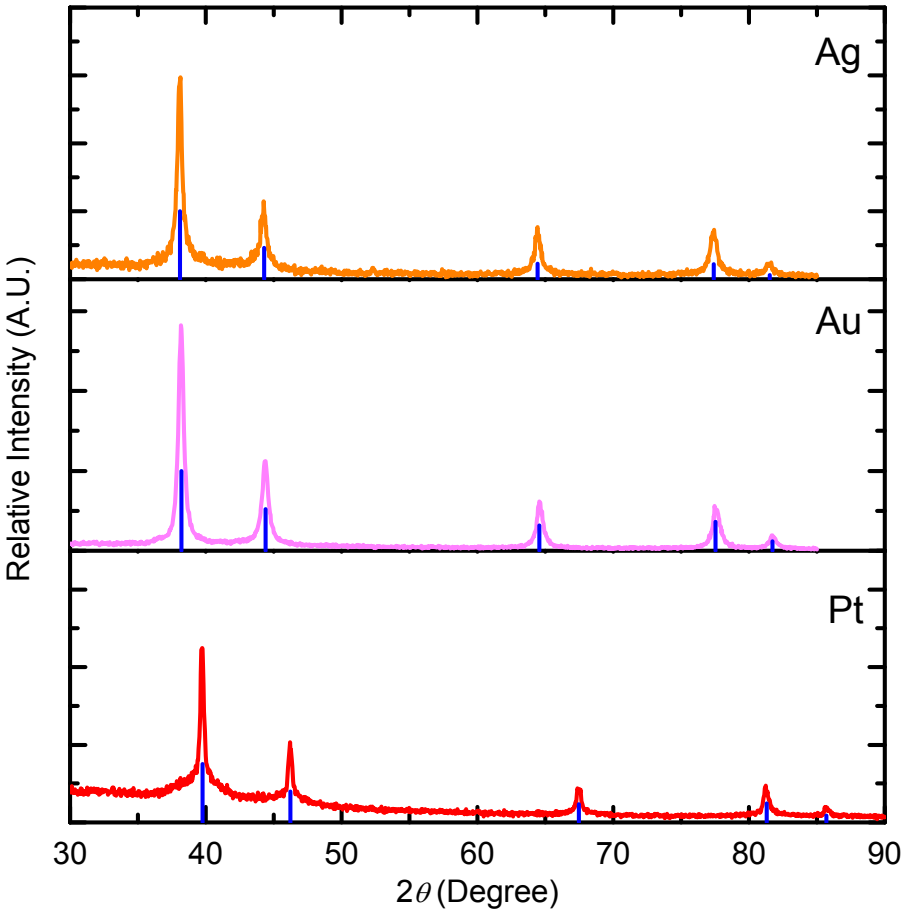

TEM of NPs:

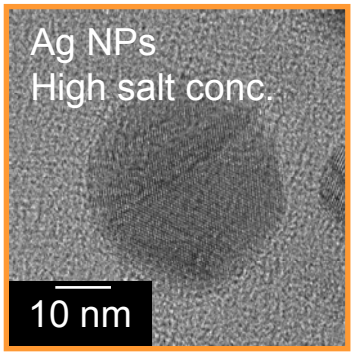

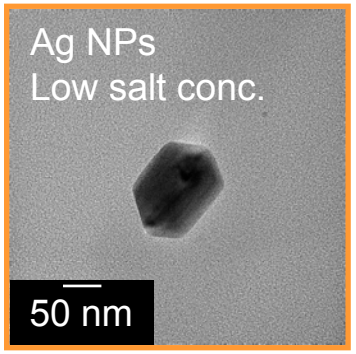

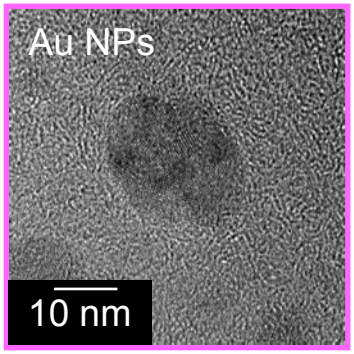

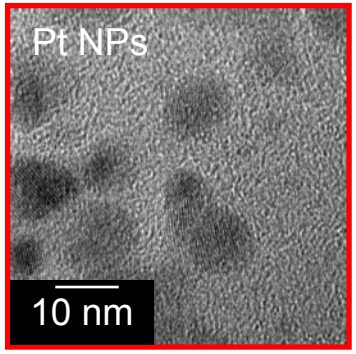

Flexible polymeric films with patterned metal nanoparticles

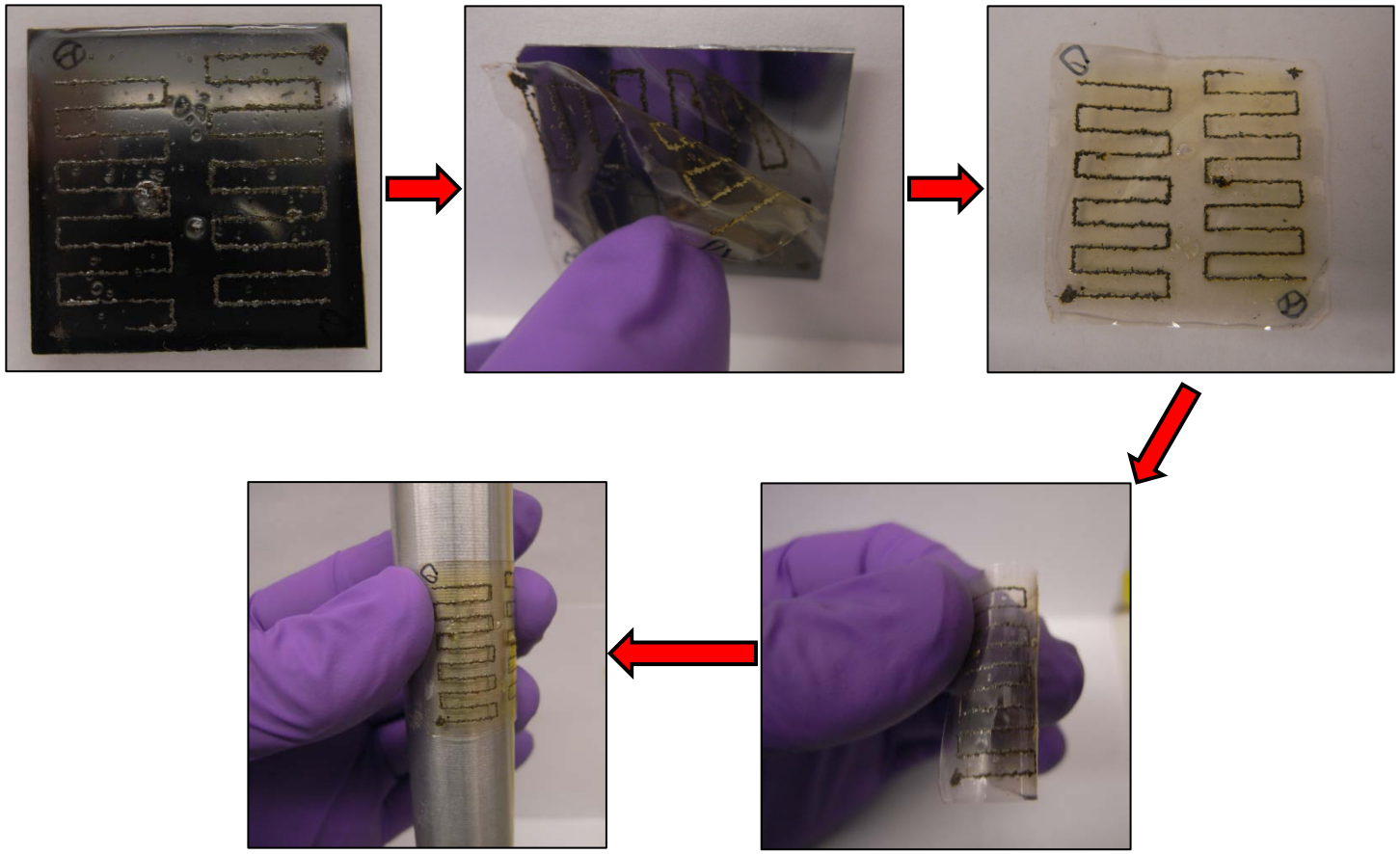

Acknowledgments

Past group members

•Dr. Wei-Hung Chiang (Post Doc, AIST, Japan)

•Matthew Cochey (Product engineer, Venture Lighting)

•Christopher Carach (Ph.D. candidate, UCSB)

Current group members

•Pin Ann Lin (Ph.D. candidate)

•Seung Whan Lee (Ph.D. candidate)

•Carolyn Richmonds

•Tessie Panthani

•Raymond Rodgers

•Trent Hovis

•Megan Witzke

•Albert Xue

Metal nanoparticle synthesis and characterization

•Amir Avishai (Materials Science)

•Prof. Frank Ernst (Materials Science)

Carbon nanotube characterization

•Regan Silvestri (Macromolecular Science)

•Prof. Jack Koenig (Macromolecular Science)

•Prof. Liming Dai (Chemical Engineering)

•Prof. Ken Singer (Physics)

FET fabrication and testing

•Mohammed Sakr (Physics)

•Prof. Xuan Gao (Physics)

Mentors

•C.C. Liu

•John Angus

Funding:

AIR FORCE OFFICE OF SCIENTIFIC RESEARCH
UNITED STATES AIR FORCE

BRIDGING THE GAP
1958 DARPA 2008
50 YEARS
POWERED BY IDEAS

NSF

CASE WESTERN RESERVE UNIVERSITY
CASE SCHOOL OF ENGINEERING

Microplasmas contain a high concentration of energetic electrons (> 10 eV)

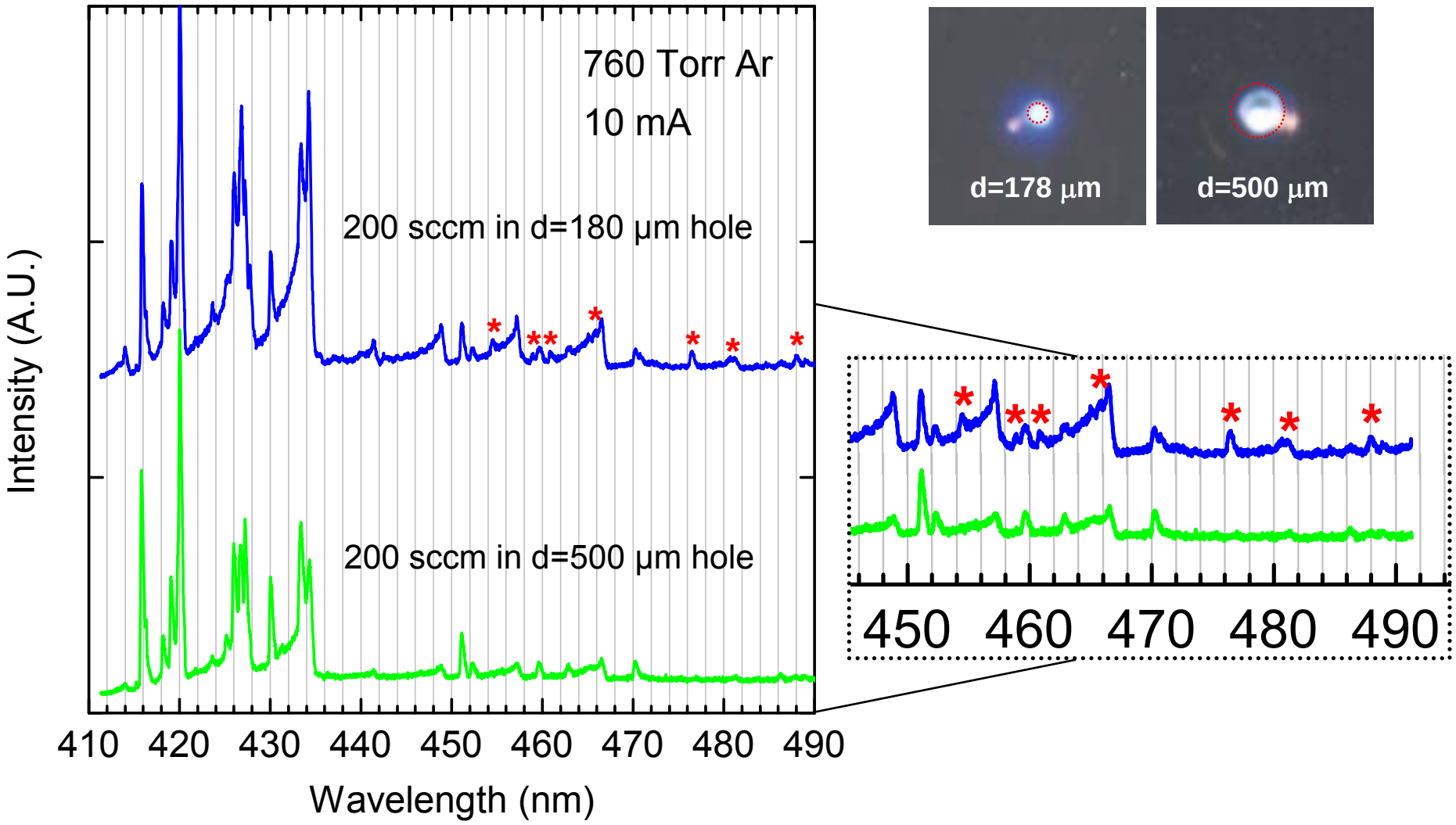

Differential mobility analysis of aerosol nanoparticles

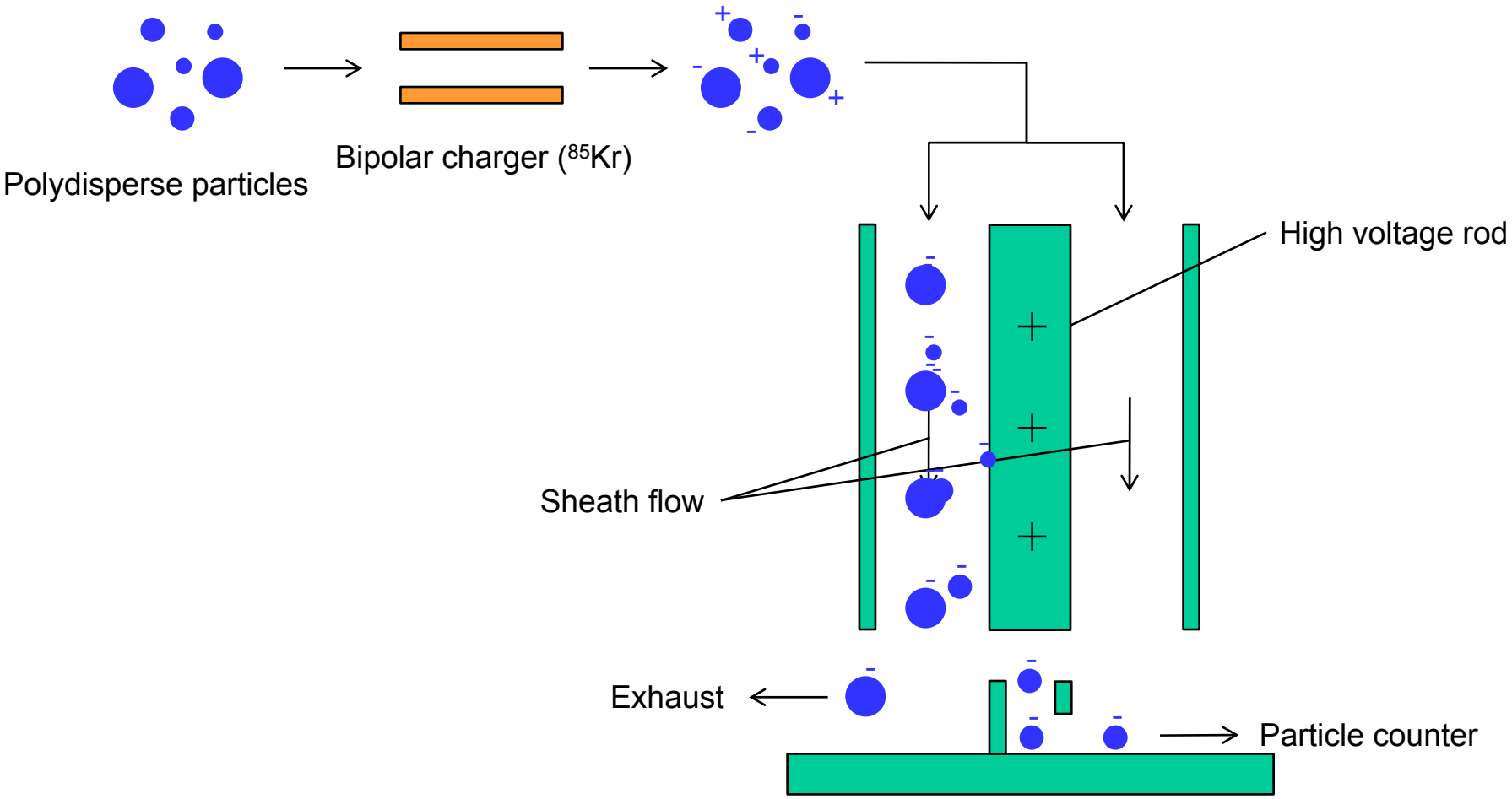

Emerging applications of nanomaterials

Nanoelectronics:

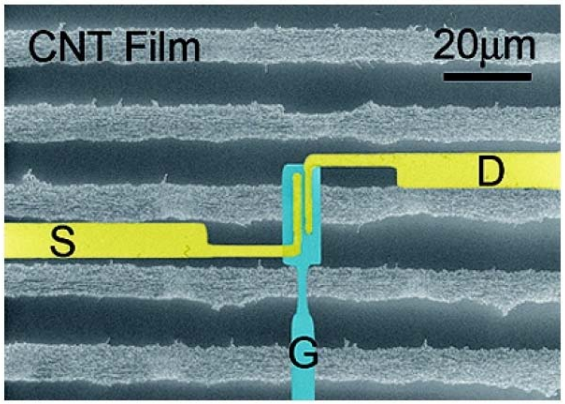

Avouris, ACS Nano (2008)

Catalysis:

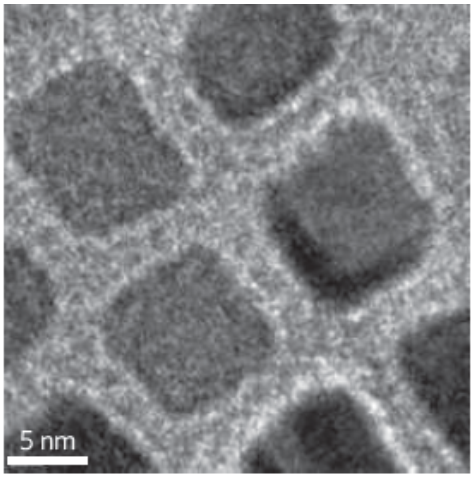

Roy, Mater. Lett. (2006)

Nanomedicine:

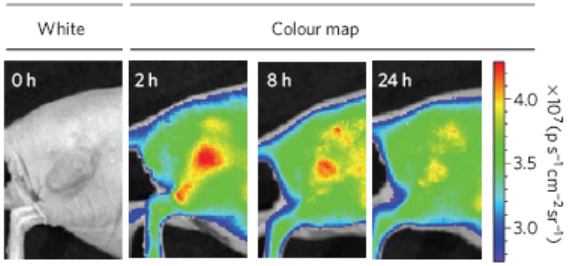

Sailor, Nature Materials (2009)

Solar energy conversion:

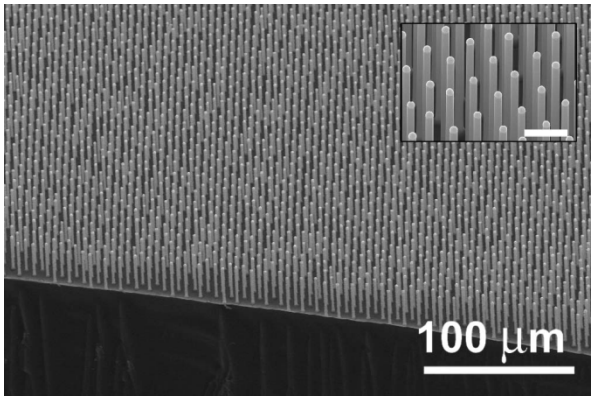

Atwater, APL (2007)

Aerosol size classification of CNTs catalyzed by Fe and Ni NPs

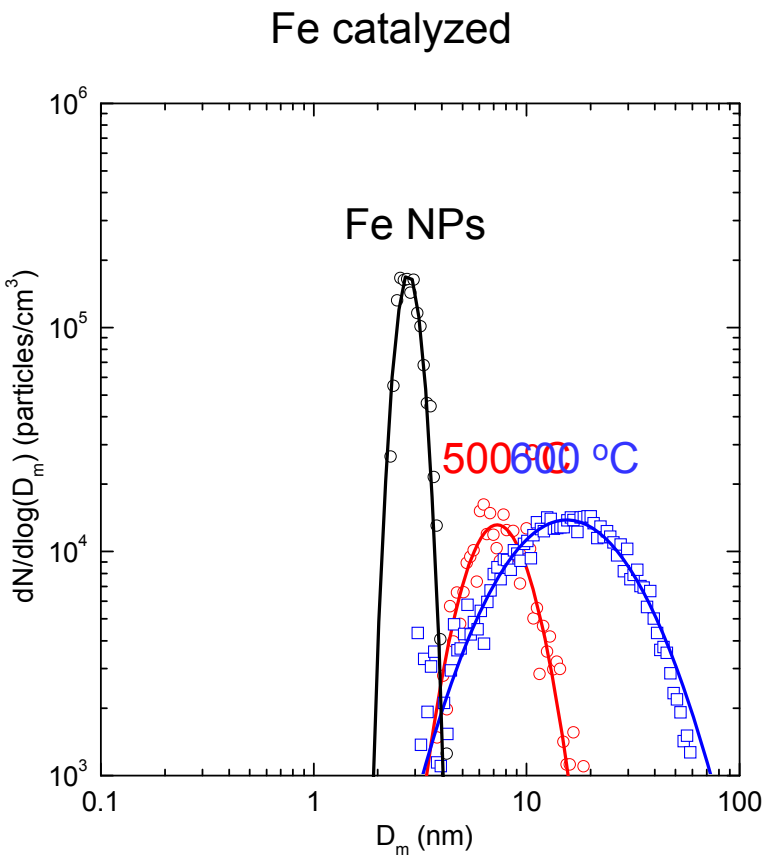

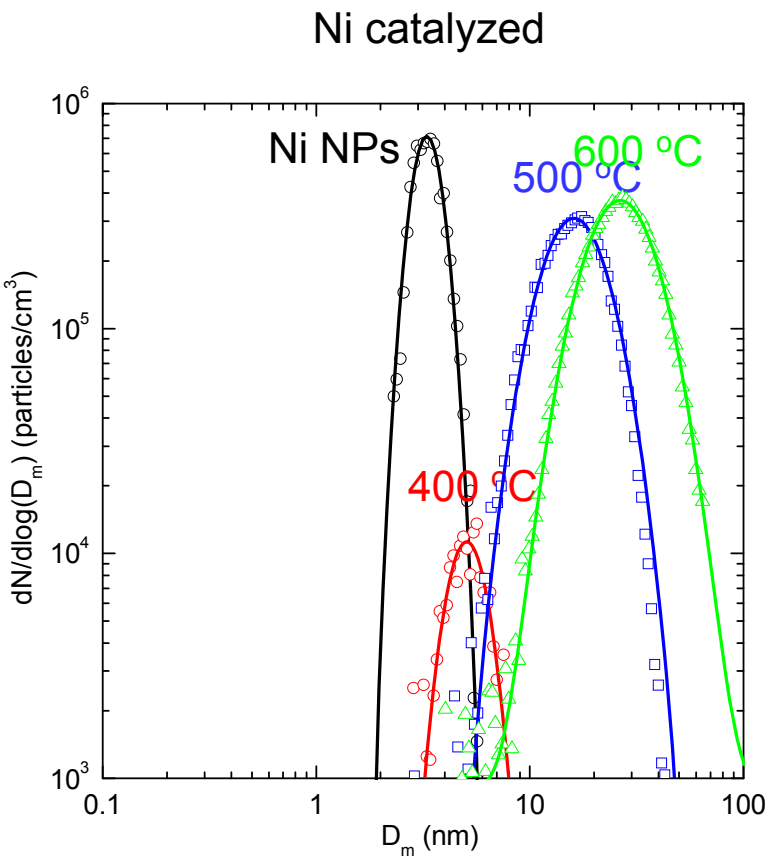

HRTEM analysis of carbon nanostructures

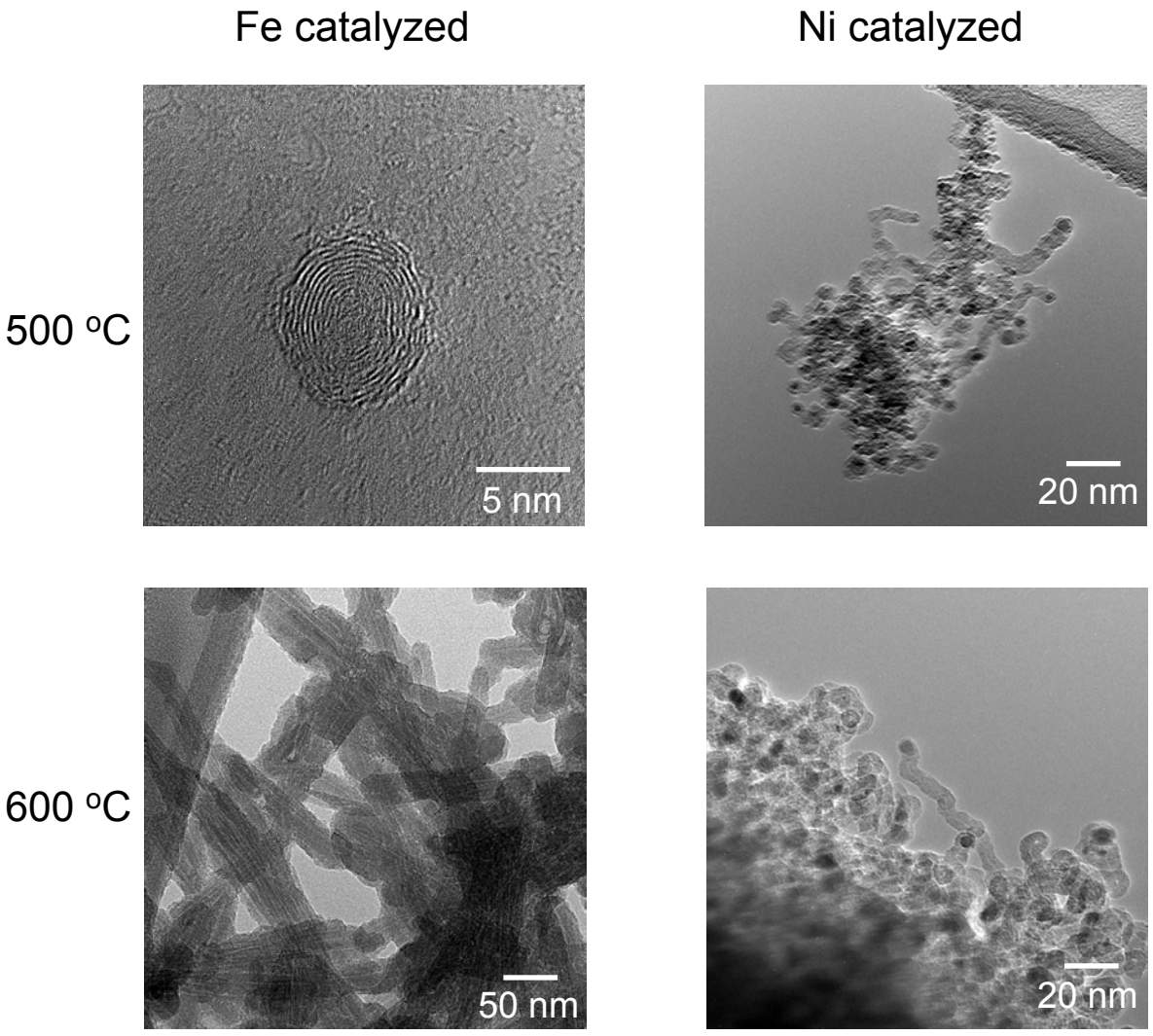

Extracting kinetic parameters for CNT growth from aerosol measurements

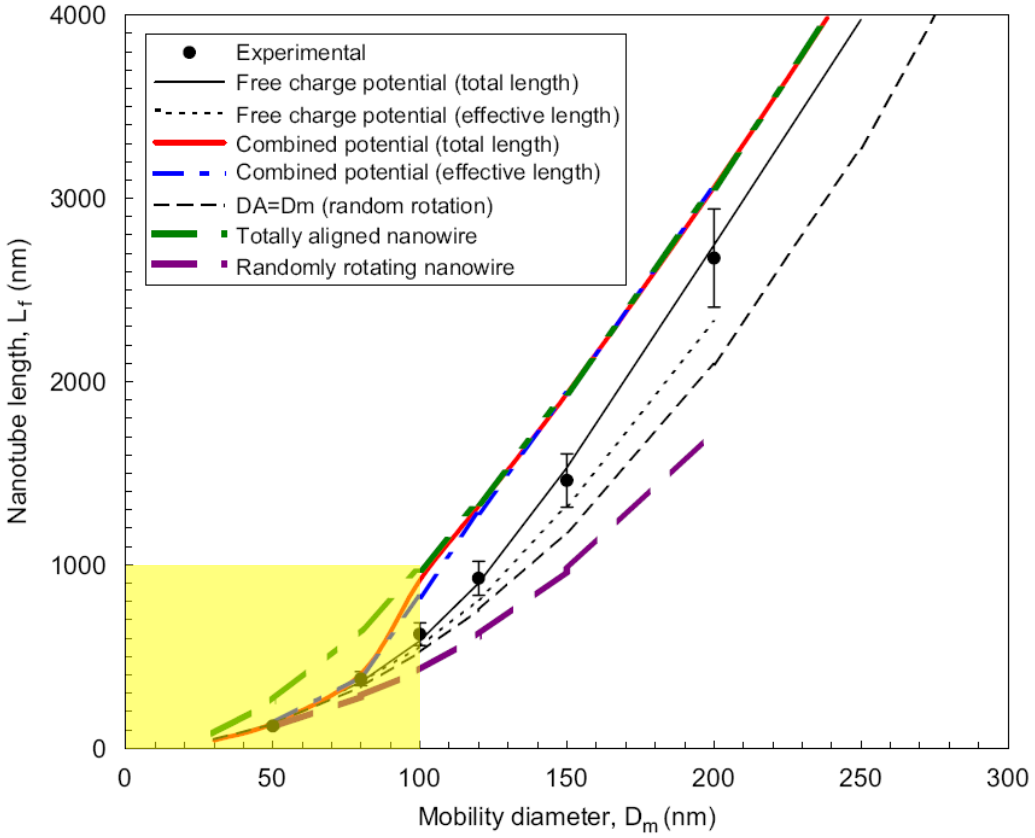

S.H. Kim *et al.,* J. Aerosol Sci., Vol. 38, 823 (2007)

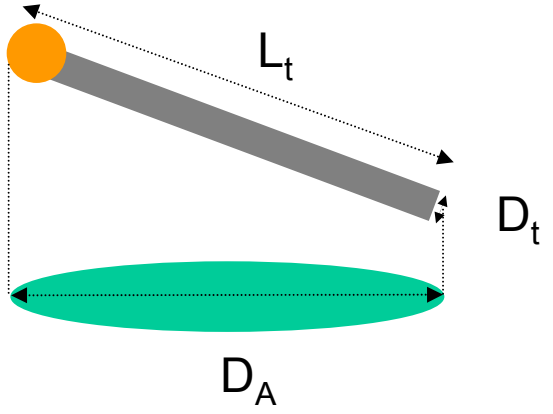

►Electrical mobility diameter (D_m) corresponds to projected area diameter (D_A)

CNT length calculation:

$$L_t = \frac{\pi D_m^2}{4 D_t}$$